WATER SCIENCE SERIES

An Overview of LiDAR for Watershed Applications in British Columbia

Daniel Lamhonwah, Erin Seagren, Robin Pike

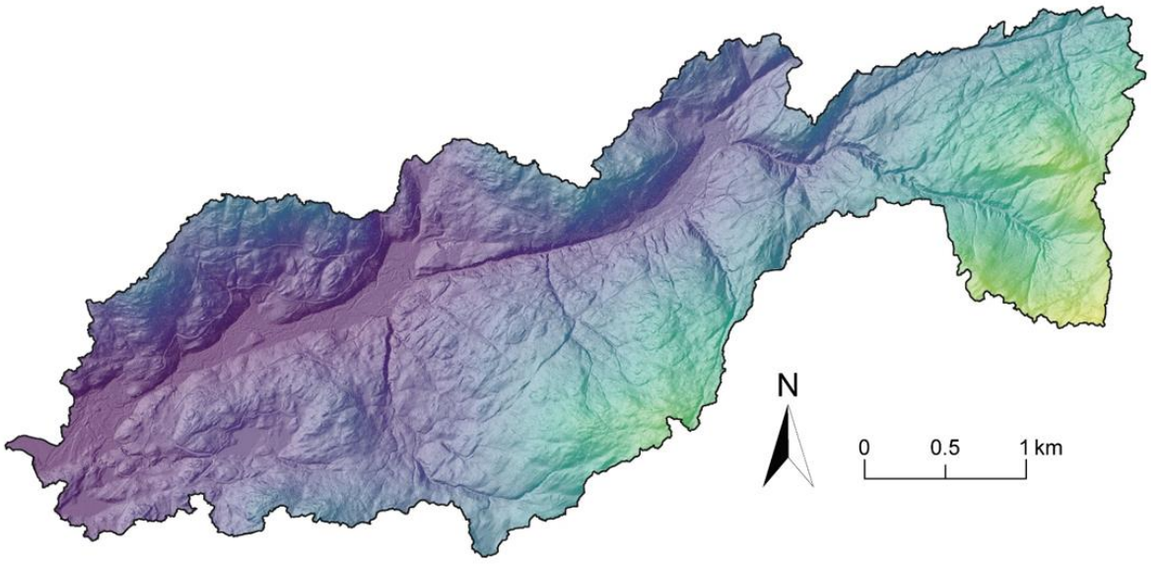

July 2025

BRITISH COLUMBIA

No. 2025-07

The **Water Science Series** are scientific technical reports relating to the understanding and management of B.C.'s water resources. The series communicates scientific knowledge gained through water science programs across B.C. government, as well as scientific partners working in collaboration with provincial staff. For additional information visit: http://www2.gov.bc.ca/gov/content/environment/air-land-water/water/water-science-data/water-science-series.

ISBN: 978-1-0399-0158-2

Citation:
Lamhonwah, D., E.G. Seagren and R.G. Pike, 2025. An Overview of LiDAR for Watershed Applications in British Columbia. Water Science Series, WSS2025-07. Province of British Columbia, Victoria.

Authors' Affiliation:
Daniel Lamhonwah, Ph.D., P. Ag
Watershed Hydrologist
B.C. Ministry of Water, Land and Resource Stewardship
2975 Jutland Road, Victoria B.C., V8T 5J9

Erin G. Seagren, Ph.D.
Watershed Geomatics Specialist
B.C. Ministry of Water, Land and Resource Stewardship
200-10470 152nd Street, Surrey B.C., V3R 0Y3

Robin G. Pike, M.Sc., P. Ag
Watershed Science Hydrologist
B.C. Ministry of Water, Land and Resource Stewardship
2975 Jutland Road, Victoria B.C., V8T 5J9

Cover Photograph:
Digital Elevation Model (DEM) of the Carnation Creek Watershed, B.C. derived from LiDAR (2023).

ACKNOWLEDGEMENTS

The authors thank the following people for their comments, which greatly improved this report (in alphabetical order): Alexandre Bevington (Restoration and Research – Omineca Region, Ministry of Forests); Amanda Girard (Regional Operations Division - Coast Area, Ministry of Forests); Julie Ann Ishikawa (Watershed Stewardship and Security Branch, Ministry of Water, Land and Resource Stewardship); Taylor Josephy (Watershed Stewardship and Security Branch, Ministry of Water, Land and Resource Stewardship); Tom Millard (Regional Operations Division - Coast Area, Ministry of Forests); Jeremy Morris (Watershed Stewardship and Security Branch, Ministry of Water, Land and Resource Stewardship); Sasha Nasonova (Forest Analysis and Inventory Branch, Ministry of Forests), Hunter Rigatti (Watershed Stewardship and Security Branch, Ministry of Water, Land and Resource Stewardship); and Mike Shasko (GeoBC Branch, Ministry of Water, Land and Resource Stewardship).

CONTENTS

FIGURES

ACRONYMS

ALS	Airborne laser scanner
CHM	Canopy Height Model
DEM	Digital Elevation Model
DoD	Digital surface model of difference
DSM	Digital Surface Model
DTM	Digital Terrain Model
FWA	Freshwater Atlas
GIS	Geographic Information System
GNSS	Global Navigation Satellite System
HAND	Height Above Nearest Drainage
IMU	Inertial measurement unit
LiDAR	Light Detection and Ranging
QAQC	Quality Assurance and Quality Control
REM	Relative Elevation Model
TRIM	Terrain Resource Information Management
UAV	Unmanned aerial vehicle

1. INTRODUCTION

In recent years, the availability of airborne LiDAR (Light Detection and Ranging) products have increased rapidly. As a subset of remotely sensed data, LiDAR has been widely used across the fields of forestry, archaeology, agrology, ecology, geoscience, and emergency management. In watershed management, LiDAR is used to create a detailed spatial foundation for basin analysis and characterization. In general, watershed characterizations were limited by a lack of detailed spatial data to help fully understand a watershed's history, composition, and functioning. In the present, LiDAR presents an opportunity to help fill this information gap.

LiDAR's strength lies in its ability to remove most vegetation from the terrain with a very high level of detail and provide wide-area information, thus enhancing field investigations. While not a direct substitute for on-the-ground work, it helps users better understand a watershed when combined with other tools and methods. High-resolution LiDAR data can provide detailed and accurate information on fundamental watershed characteristics such as watershed boundaries, surface features, flow paths, slope, channel morphology, sub-canopy disturbances, seasonal snow cover changes, topography and other uses (Jones et al., 2008; Höfle and Rutzinger, 2011; Petroselli, 2012). Further, LiDAR data has been used to examine watershed processes affected by stressors such as drought, wildfire, and land use change, and subsequent effects on water availability and quality (Hagemann, et al., 2013; Chawla et al., 2020; Yang et al., 2021).

This report aims to introduce readers to basic LiDAR concepts and derivative products useful for watershed applications. It defines common LiDAR terms and uses visualizations to aid in comprehension. The objective is to equip readers with foundational LiDAR knowledge and terminology, to explore its potential application in their watershed(s) of interest, and to facilitate discussions with others. This report does not provide technical guidance on how to use LiDAR.

2. LIDAR BACKGROUND

2.1 What is LiDAR?

LiDAR (Light Detection and Ranging) is a remote sensing technology that gathers information about objects or areas from a distance without direct contact (Figure 1). LiDAR emits pulsed laser light and measures the time it takes for that light to return to calculate distances between the object and the detector (ESRI, 2021). A common application is mapping the Earth's surface using airborne LiDAR, which involves an airborne laser scanner (ALS) mounted on a plane or unmanned aerial vehicle (UAV – also known as a drone).

An ALS principally includes a laser, a scanner, a detector, ground control points, Global Navigation Satellite System (GNSS), and an inertial measurement unit (IMU). The laser typically emits light in the near-infrared spectrum (i.e., is not visible, electromagnetic, etc.). This light is reflected by objects, collected by the scanner and sent to the detector (Figure 1). This results in multiple returns to the aircraft, caused by scattering of the laser pulse. The detector in the aircraft collects time data and calculates distance. This information combined with aircraft position from the GNSS receiver, then generates a point cloud data set. (See: Section *2.2 What is a point cloud?*).

To ensure accurate positioning of collected LiDAR data by the ALS, ground control points (physical markers placed in locations on the Earth’s surface with known easting, northing, and elevation coordinates, and that are distinctly visible in the point cloud) are used as reference points to aid georeferencing of LiDAR data. The aircraft’s GNSS receiver collects positioning measurements from

satellite constellations, which along with ground control points, correct elevations. The aircraft's IMU adjusts for orientation and a ground-based real-time kinematic (RTK) positioning system, which is part of the GNSS, provides further position corrections to ensure data accuracy.

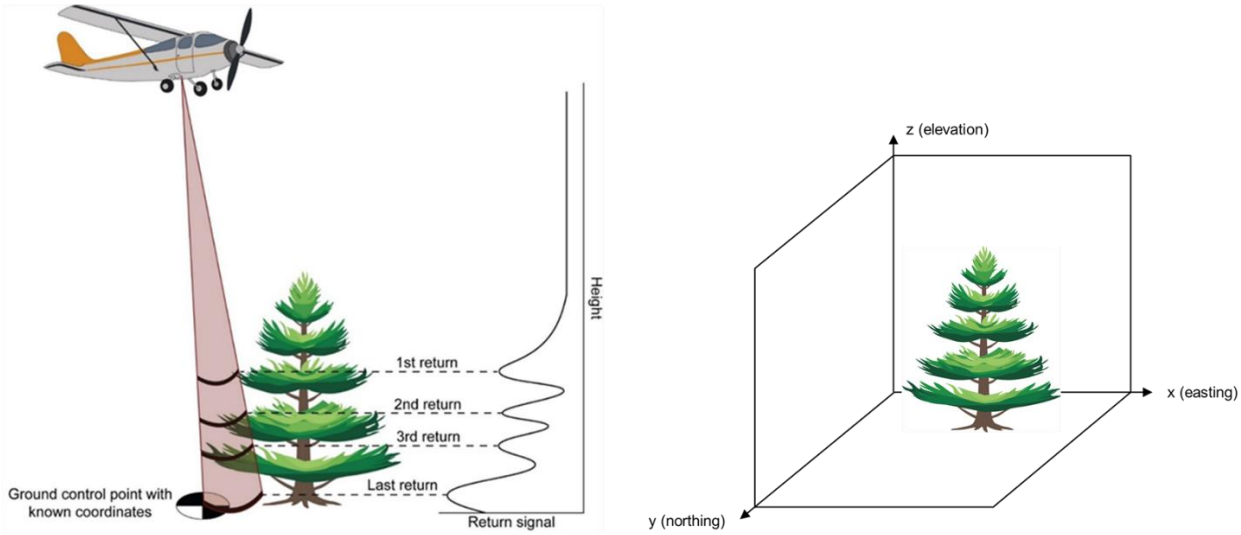

Figure 1: (A) Visualization of airborne LiDAR data collection system. (B) LiDAR data points consist of easting (x), northing (y) and elevation (z) coordinates.

2.2 What is a point cloud?

Data from the ALS generates a dense array of data points known as a 'point cloud'. Each point in the cloud represents a location on the Earth's surface with projected coordinates (easting, northing, and elevation), a timestamp, and other attributes (e.g., scan angle, scan direction, return count, intensity) (GeoBC, 2023). Points in a point cloud collectively form a 3D representation of the Earth's surface including natural features (e.g., trees, bedrock outcrops) and constructed objects (e.g., buildings, roads, powerlines). Figure 2 shows a very dense point cloud cross section of LiDAR data collected in the Carnation Creek Watershed (Vancouver Island, B.C.). Using specialized LiDAR software, point cloud data (saved as a .las or .laz file) can produce derivative products such as Digital Elevation Models (DEMs), Digital Surface Models (DSMs), contour maps, and watershed delineation maps (See: Section *3. LiDAR Derivative Products*).

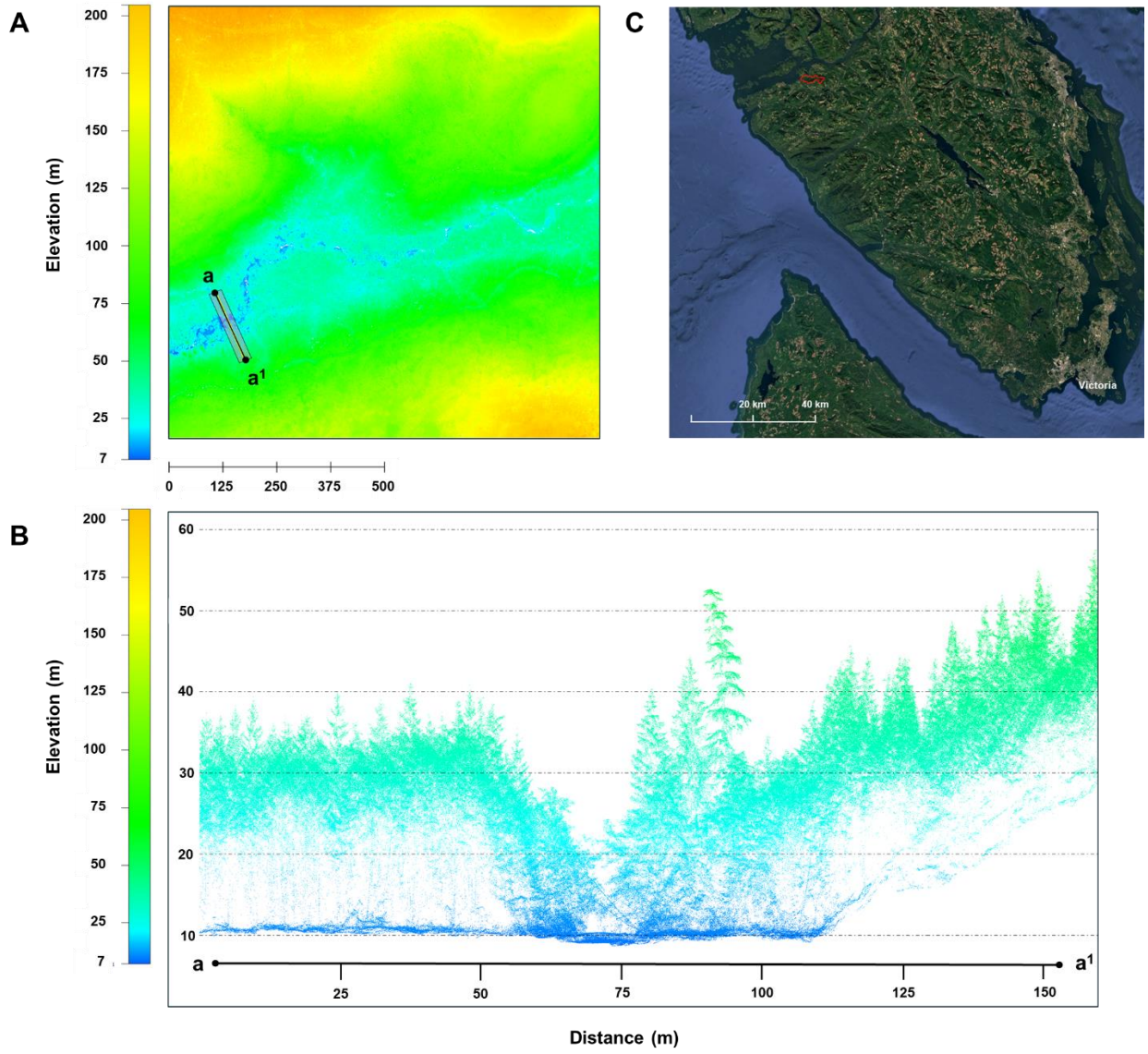

Figure 2: A 2023 point cloud at the Carnation Creek Watershed, B.C. contains about 10 million ground surface and vegetation data points. Figure (A) shows a planimetric view (looking down) of ground elevation within the Carnation Creek Watershed, B.C. Figure (B) shows a side view along a cross-section (a to a[1]) illustrating tree canopy structure. The colors in (A) and (B) indicate elevation, ranging from 7 m to just over 200 m above sea level. Figure (C) shows the location of the Carnation Creek Watershed (outlined in red) on the west coast of Vancouver Island.

2.3 What are the advantages to using LiDAR for watershed characterization?

Airborne LiDAR provides spatial data over a large geographic area. Depending on the point density and canopy type, LiDAR pulses can make their way through gaps in the canopy to the forest floor. LiDAR data users can visually identify features like forestry roads, gullies, floodplains, and stream channels in LiDAR derivative products. The visibility of features depends on the product's spatial resolution. Figure 3 shows the difference in detail between a 20-cm resolution Digital Elevation Model (DEM) and a 25-m resolution Terrain Resource Information Management (TRIM) image of the same watershed, at the same scale. The

high-resolution DEM (Figure 3A) more clearly distinguishes roads and gullies unlike the coarser resolution TRIM image (Figure 3B).

One key advantage of LiDAR over other remote sensing technologies is the ability to collect surface elevation data under vegetation which isn't visible using traditional aerial imagery (NOAA Coastal Services Center, 2012). It should be clarified that optical LiDAR does not penetrate directly through vegetation, rather, LiDAR measures through the openings between leaves, needles and branches to the ground surface, where it reflects back to the aircraft scanner (NOAA Coastal Services Center, 2012). However, in areas with dense vegetation canopies or understories, data density may be insufficient for accurate ground visualization.

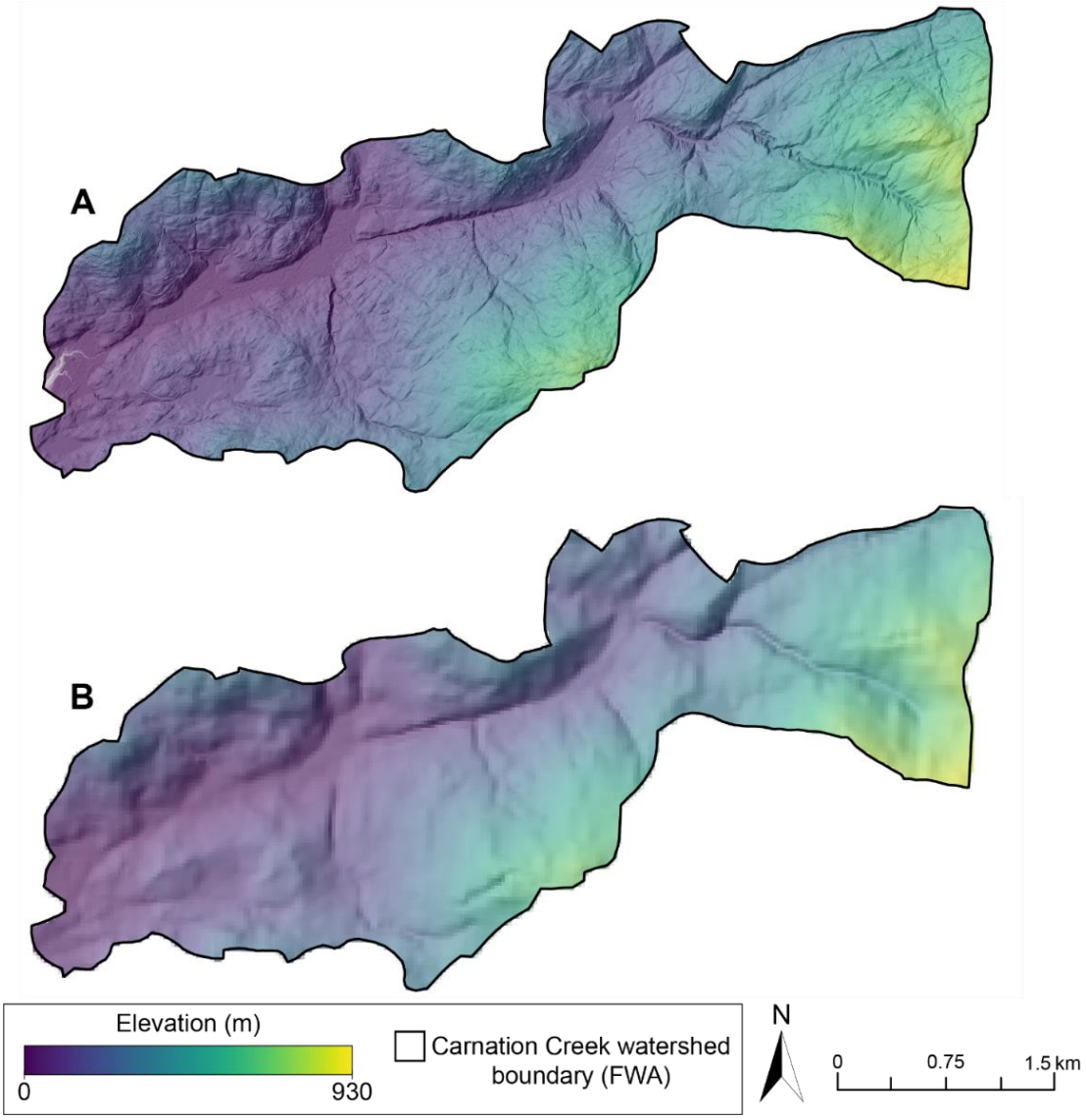

Figure 3: Comparison of a 20-cm vs. 25-m DEM's for the Carnation Creek Watershed, B.C. (A) LiDAR 20-cm DEM and hillshade (B) TRIM 25-m DEM and hillshade. Both images use the BC Freshwater Atlas watershed boundary.

Conventional LiDAR is limited in seeing through water, with penetration effective only to a few tens of centimeters (or less) below the surface as infrared light is strongly absorbed by water (Reusser and Bierman, 2007; Cavalli et al., 2008; Notebaert et al., 2009). For water applications, green LiDAR, which uses water penetrating green light is used for bathymetric mapping (Kinzel et al., 2013). Green LiDAR systems are flown at lower altitudes compared to conventional LiDAR used for land surface mapping (Szafarczyk and Toś, 2022). Reviews of green LiDAR indicate under ideal conditions (e.g., clear water minimal turbidity, no waves or ripples) it can penetrate tens of metres below the water surface (Szafarczyk and Toś, 2022). Maximum depth varies with turbidity, water surface roughness, aquatic vegetation, and bottom reflectance.

2.4 General Quality Assurance and Quality Control (QAQC) Workflow

Quality Assurance and Quality Control (QAQC) ensures that LiDAR data meets quality goals, which is crucial for accurately representing the physical environment in derivative products (see Section *3: LiDAR Derivative Products*). Figure 4 presents one of many QAQC pathways for LiDAR data, providing a general workflow of the QAQC process, including starting points and general steps. Note: a typical QAQC process is not always linear as users may start at different steps, skip steps, or revisit steps. Additionally, as a QAQC summary, there are many detailed steps not described under the general workflow presented below that may be required.

- **Step 1. Data collection:** Airborne LiDAR data are collected using laser scanners (ALS) mounted to a plane, helicopter, or UAV. This data generates a dense array of points called a point cloud.
- **Step 2. Data calibration and georeferencing:** LiDAR data calibration ensures accuracy and consistency by correcting for internal and external errors (e.g., scanner/sensor noise from temperature changes or electronic interference). Georeferencing adds coordinate information to a point, accurately representing it on a map (i.e., the digital point accurately represents a physical point on the ground).
- **Step 3. Point classification:** Every point in a LiDAR point cloud can be classified by the type of object that reflected the laser pulse (e.g., ground, vegetation, building, water etc.). LiDAR software can automatically classify points, but manual classification may also be an option or desired.
- **Step 4. Publication and use of data:** Data that meets quality goals (accurately georeferenced and classified) can be used to develop derivative products like DEM's. These products can be published for public access on platforms such as LidarBC's Open LiDAR Data Portal.

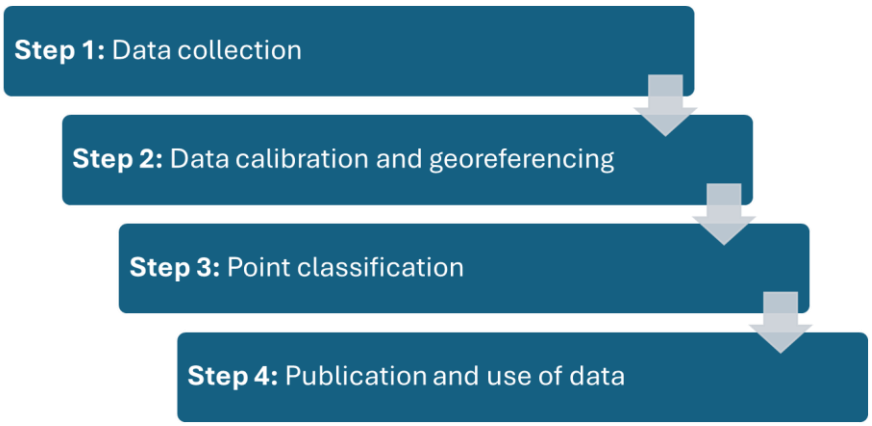

Figure 4: LiDAR data Quality Assurance Quality Control (QAQC) workflow.

2.5 Where can LiDAR data for British Columbia be accessed?

Over the past several years, the Government of B.C. has increased investments in the collection of LiDAR across B.C. and created a repository under the Open Government License, making it freely accessible to download and use. BC LiDAR data can be accessed using LidarBC's Open LiDAR Data Portal. Alternatively, LiDAR data can also be accessed via the Open LiDAR Data Portal – Web Map on ArcGIS Online. *GeoBC* oversees LidarBC and manages geospatial information and products to help manage B.C.'s natural resources. B.C. is investing in a six-year program to collect high-resolution, publicly accessible LiDAR elevation data for the entire province.

The typical resolution of LiDAR-derived DEMs available from LidarBC is between 1- to 2-m. However, data users with access to LiDAR processing software can download point cloud data to create higher-resolution DEMs or investigate the canopy if the point density is sufficient.

Some cities, municipalities, and regional districts in B.C. also provide publicly accessible LiDAR data. For example, the City of Vancouver provides LiDAR data via the Open Data Portal. The City of Surrey provides LiDAR data via the Bulk Data repository and the Municipality of North Cowichan via BC Data Catalogue. LiDAR derivative products for other areas of B.C. are also available from the Government of Canada's Open Government website.

LiDAR data for parts of B.C. are available from OpenTopography, a geospatial data repository run by the UC San Diego, Arizona State University, and the EarthScope Consortium. For more LiDAR sources, please check government and academic data repositories.

2.6 What are the requirements and challenges of using LiDAR?

While LiDAR is a valuable resource for various assessments, it is important to understand its requirements and challenges. This report outlines several requirements and limitations relating to LiDAR data collection, processing, and derivative product generation. This discussion is not exhaustive. Further, detailed costs associated with the collection of LiDAR data are not covered, assuming readers will be using freely accessible LiDAR data.

2.6.1 Specialized software and hardware for LiDAR data processing is required

LiDAR processing often requires third-party software and specialized training. Both free and commercial programs are available for processing point clouds and creating derivative products. Common commercial Geographic Information System (GIS) products include ESRI ArcGIS and Global Mapper. A free option includes QGIS. Further, a variety of Python packages like LAStools, Whitebox Tools, laspy and R packages such as lidR are freely available but require programming language skills.

2.6.2 LiDAR data storage and processing requirements

LiDAR data often requires significant computer storage; where files for large watersheds can exceed several hundred gigabytes. High performance hardware (e.g., fast processors, ample RAM, and graphics cards) are required to enable efficient data processing. Data hosting and sharing solutions (e.g., a LAN, cloud storage, FTP, portable drives) are also important due to the large storage capacity requirements.

2.6.3 Spatial data completeness

Spatial data completeness refers to how fully LiDAR data covers an area. Data gaps can occur due to flight errors (unscanned areas or insufficient spacings of flight lines), equipment malfunctions, poor weather (e.g., fog, clouds, rain, haze, smoke, etc.) or operation in a restricted airspace (e.g., in no-fly zones, over private property). Data gaps can also occur if the distance between flight lines or the flight height above the ground varies during collection (Gatziolis and Andersen, 2008). Additionally, watershed

boundaries are not typically used to plan LiDAR data acquisitions, and as such, watershed boundaries and stream networks may be difficult to resolve with incomplete data.

2.6.4 Spatial resolution considerations

Point cloud density and the number of ground returns (i.e., laser pulses that hit and return from the ground surface) determine the resolution of LiDAR data and derivative products. Insufficient point cloud density can lead to resolution issues in derivative products. For example, a LiDAR generated DEM with 25 m pixels won't accurately capture features smaller than 625 m^2. Therefore, it is important to first consider the required resolution (scale) in relation to project objectives.

2.6.5 Time and frequency of data acquisition

LiDAR data captures a 'snapshot' of environmental conditions and topography at the time of collection. A single snapshot can be limiting if conditions or topography change after LiDAR data collection (e.g., landsides), especially if project focus is on those changes. In such cases, the data would not reflect current conditions and would not provide an up-to-date characterization.

It is important to consider project objectives prior to the use of LiDAR data to ensure the timeline of data collection is appropriate. Similarly, for time series change detection, the required time intervals between LiDAR data sets depend strongly on project objectives and the availability of LiDAR data, which ideally align. Change detection in remote sensing involves analyzing changes in the same area over time. For example, snow accumulation and melt monitoring may require LiDAR data to be collected every 2 to 4 weeks, while glacier retreat studies may require data collected years apart.

3. LIDAR DERIVATIVE PRODUCTS

A LiDAR derivative product is information, often visualized as a map, that has been developed from a LiDAR dataset (i.e., point cloud). The following sections provide examples of LiDAR derivative products for various watershed-related applications. These examples aim to illustrate how LiDAR can help achieve goals and objectives in different watersheds.

3.1.1 Digital Elevation Model (DEM)

A Digital Elevation Model (DEM) is a 3-dimensional representation of the surface of the Earth (i.e., a bare-earth representation), excluding any natural or constructed features such as trees and buildings, but often including roads (Ministry of Water, Land, and Resource Stewardship, 2024). To create a DEM, software extracts ground points from a point cloud and interpolates a continuous, 3D representation of the Earth's surface. Figure 5 shows: (A) a high resolution (20-cm) DEM and hillshade of the Carnation Creek Watershed, (B) a research station in the lower watershed and (D) a portion of the Carnation Creek mainstem located mid-watershed. While significant tree cover is apparent in both orthoimages (Figures 5C and 5E), the DEM demonstrate how LiDAR can be used to detect the underlying topography.

DEMs are typically stored as rasters, with data represented by a consistent-sized grid of cells, each containing a value (e.g., elevation). For a given area, the greater the number of cells in a matrix, the higher the spatial resolution of the corresponding DEM.

DEMs help users understand the watershed topography, identifying fluvial features (e.g., channels, terraces, and floodplains) and surficial features like bedrock outcrops (Moore et al., 1991; Walker and Willgoose, 1999; Garbrecht and Martz, 2000). Generating a DEM is the first step for many LiDAR products, such as contours maps, watershed boundary maps, and stream (flow network) maps. The

quality of these products depends on the DEM's spatial resolution, which is influenced by the area's size (larger areas may need coarser resolution for computing efficiency) and the dataset's point density (number of LiDAR points collected per m^2) (Wolock and Price, 1994).

Note that the term Digital Terrain Model (DTM) is sometimes used synonymously with a DEM. In the Province of B.C., a DTM is different from a DEM. A DTM is not a surface model, since its component elements are irregularly or randomly spaced mass points and are not continuous (GeoBC, 2023). As such, a surface must be derived from the DTM to create a Digital Elevation Model (DEM).

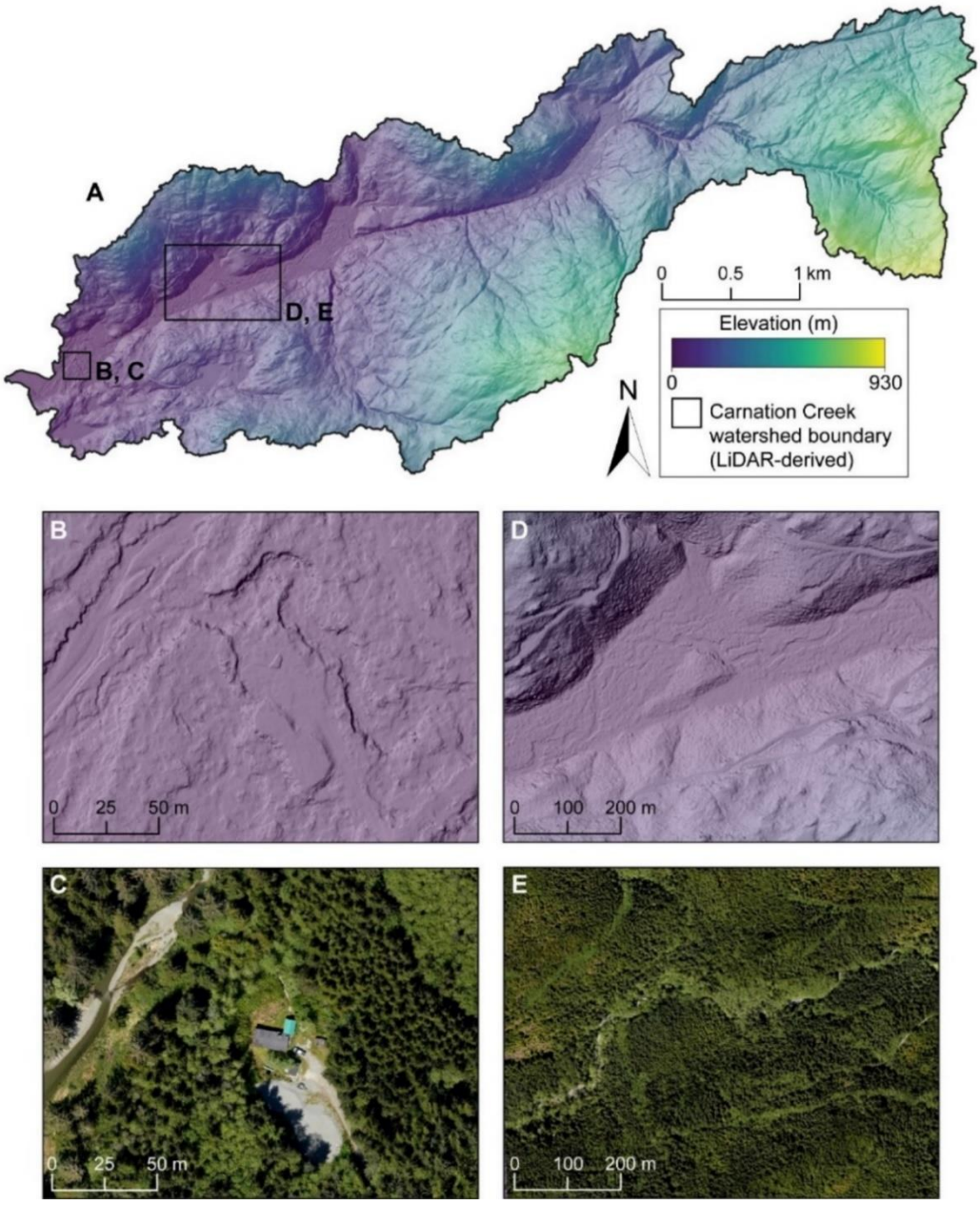

Figure 5: A) High resolution (20-cm) DEM and hillshade of the Carnation Creek Watershed. (B) research station in the lower watershed with corresponding (C) true colour orthophoto. (D) a portion of the Carnation Creek mainstem with corresponding (E) true colour orthophoto.

3.1.2 Digital Surface Model (DSM)

In contrast to a DEM, a Digital Surface Model (DSM) represents topmost features of all natural and constructed features on the Earth's surface including trees, powerlines, and buildings (Ministry of Water, Land, and Resource Stewardship, 2024). Figure 6 shows (A) a high resolution, 20-cm DSM of Carnation Creek Watershed (B) a research station in the lower watershed and (D) a portion of the Carnation Creek mainstem located mid-watershed. The DSM shows the watershed is densely vegetated, with irregular areas absent of vegetation such as buildings and roads (Figure 6B). DSMs are generally less effective than DEMs for identifying ground features like roads. Comparing the same watershed area, using a DEM and DSM (Figures 5D and 6D), access roads are more discernible in the DEM image, while in the DSM, these roads are mostly obscured by tree cover.

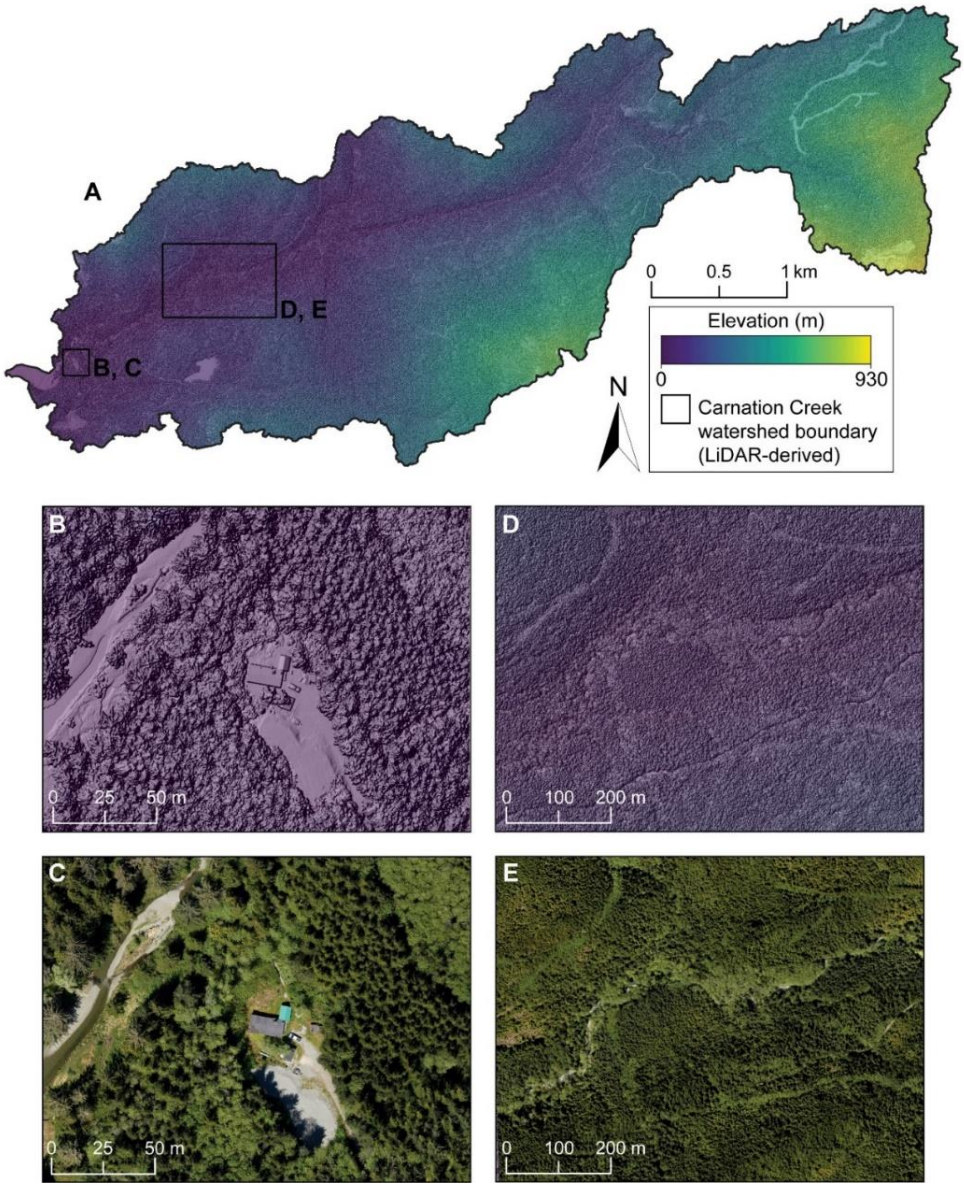

Figure 6: (A) DSM and hillshade of the Carnation Creek Watershed. (B) research station in the lower watershed with corresponding (C) a true colour orthophoto, and (D) a portion of the Carnation Creek mainstem, located mid-watershed with corresponding (E) a true colour orthophoto.

Watershed DSMs are useful for: i) flood-risk assessments (e.g., proximity of buildings to potential flood areas); ii) infrastructure planning, installation, and maintenance (e.g., powerline corridors, telecommunication towers, wind farms); iii) forestry planning (e.g., stand area, tree heights, windthrow hazard mitigation, and tree density near riparian areas); iv) land-use planning; and, v) urban modelling (Lopez and Maxwell, 2016; Münzinger et al., 2022; Priestnall et al., 2000).

3.1.3 Contour map

A contour map represents the Earth's surface using continuous lines that connect points of equal elevation (Figure 7). Contour maps can be derived from a DEM at various contour intervals, with the vertical accuracy of the DEM controlling the reliability of these intervals. The higher resolution and vertical accuracy of airborne LiDAR allows for much more detailed contour lines than from coarser DEMs such as TRIM.

A contour map helps users to understand surface characteristics such as aspect and slope in a watershed. Although, it does not show a 3D surface (e.g., a convex, concave, or linear hillslope, undulating terrain) it can be interpreted based on the shape and orientation of the contour lines (Figure 7). For example, V-shaped contour lines can indicate stream channels, where the point of the 'v' is directed upstream (Figure 7B). Terrain steepness can be interpreted based on how close contour lines are to one another or quantified (grade or degree) using measurement tools and the map's scale bar. Closely spaced contours indicate steeper areas, while widely spaced contours have gentler slopes or flat terrain (Figure 7C). Contour maps can be used to investigate mass movements (e.g., rockfalls, landslides, gullies), identify flow paths, and model drainage direction based on slope and aspect analyses (Van Den Eeckhaut et al., 2007; Leshchinsky et al., 2015; Wu and Lane, 2017).

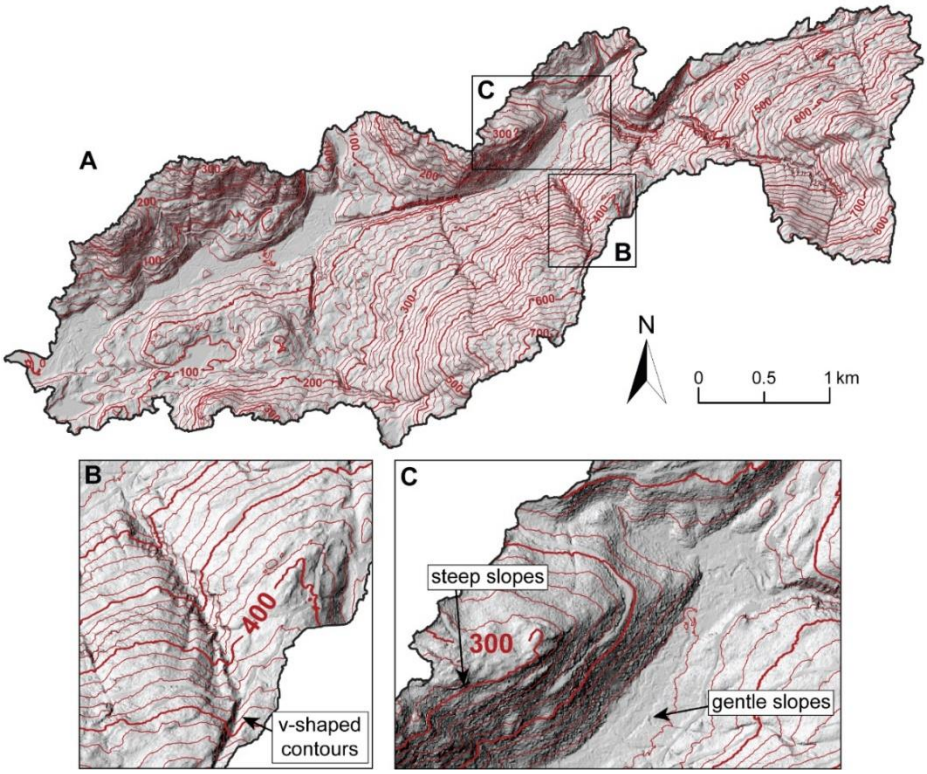

Figure 7: (A) Contour map (100 m contour intervals) of the Carnation Creek Watershed; (B) V-shaped contours indicating a stream channel; and, (C) closely spaced and widely-spaced contours indicating steep and gentle terrain.

3.1.4 Hillshade map

A hillshade map, developed from a DEM, represents the Earth's topographic surface and includes the sun's relative position to highlight features (Figure 8). Mapping software allows customization of direction, azimuth (horizon angle) and altitude (height) to control the light source location when creating a hillshade map. This helps highlight and visualize specific terrain features such as gullies, channel confinement, and flat sloped areas. Figure 8A highlights the topography of SE-facing slopes at Carnation Creek, while Figure 8B shows the topography and surficial features on NW-facing slopes. Hillshade products can also be used to map geological features such as faults which can be important to examine in groundwater studies.

In traditional single light source hillshade maps, features that are highlighted strongly depend on the light source parameters (Figure 8). In contrast, multi-directional hillshade maps combine light from multiple source directions, azimuths, and altitudes to enhance visualization of a wider variety of features. Both types of hillshades and similar texture visualizations can aid with interpreting landscape features and identifying natural features on the ground. Hillshade maps can serve as base maps, layered under other datasets to assist users understand surface expressions. In Figure 7, contour lines were layered over a hillshade map to better visualize terrain in the watershed.

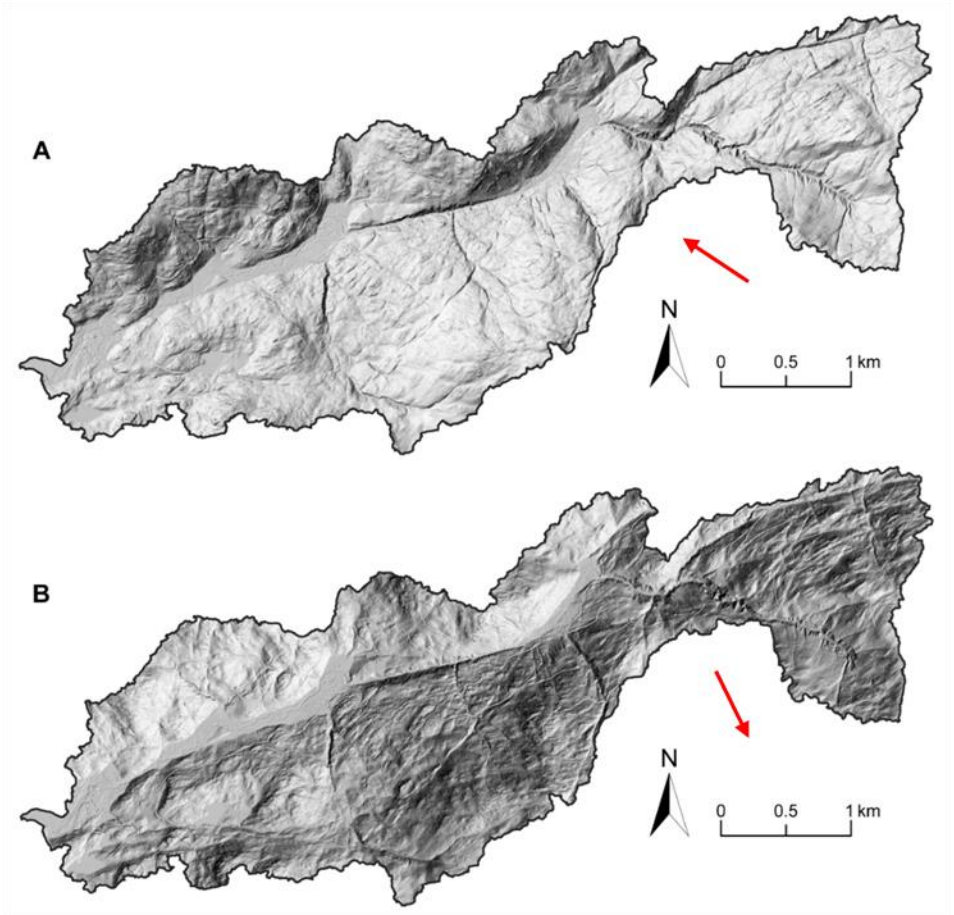

Figure 8: Two examples of Hillshade maps showing the topography of the Carnation Creek Watershed, B.C., from an azimuth of (A) 300° and (B) 120°. Note how light direction (shown as red arrows), changes highlighted features in the images.

3.1.5 Relative Elevation Model (REM)

Relative Elevation Models (REM) display elevation values relative to a distinct feature such as the local elevation of a stream channel rather than mean sea level. REMs are also known as Height Above Nearest Drainage (HAND) model. A REM is commonly created by detrending a DEM (removing the downhill trend from the data) and subtracting this detrended data layer from the bare-earth DEM (Lind, 2024). REMs are useful for flood modelling and visualizing fluvial landforms (e.g., floodplains and riparian reserves) that may be hard to discern from aerial images or DEM alone. They can also help visualize processes like sediment deposition, erosion, and channel avulsions, when multiple datasets collected at different times are available for change detection analysis (Greco et al., 2008; Hiller and Smith, 2008; Garousi-Nejad et al., 2019; Powers et al., 2019; Chen et al, 2020). Change detection analysis is further detailed in Section *3.2 Derivative Product Applications*.

Figure 9 shows a REM of the lower section of the San Juan River watershed on Vancouver Island, B.C. It visualizes the stream network and Harris Creek tributary, an unnamed oxbow lake and surface connection to Fairy Lake.

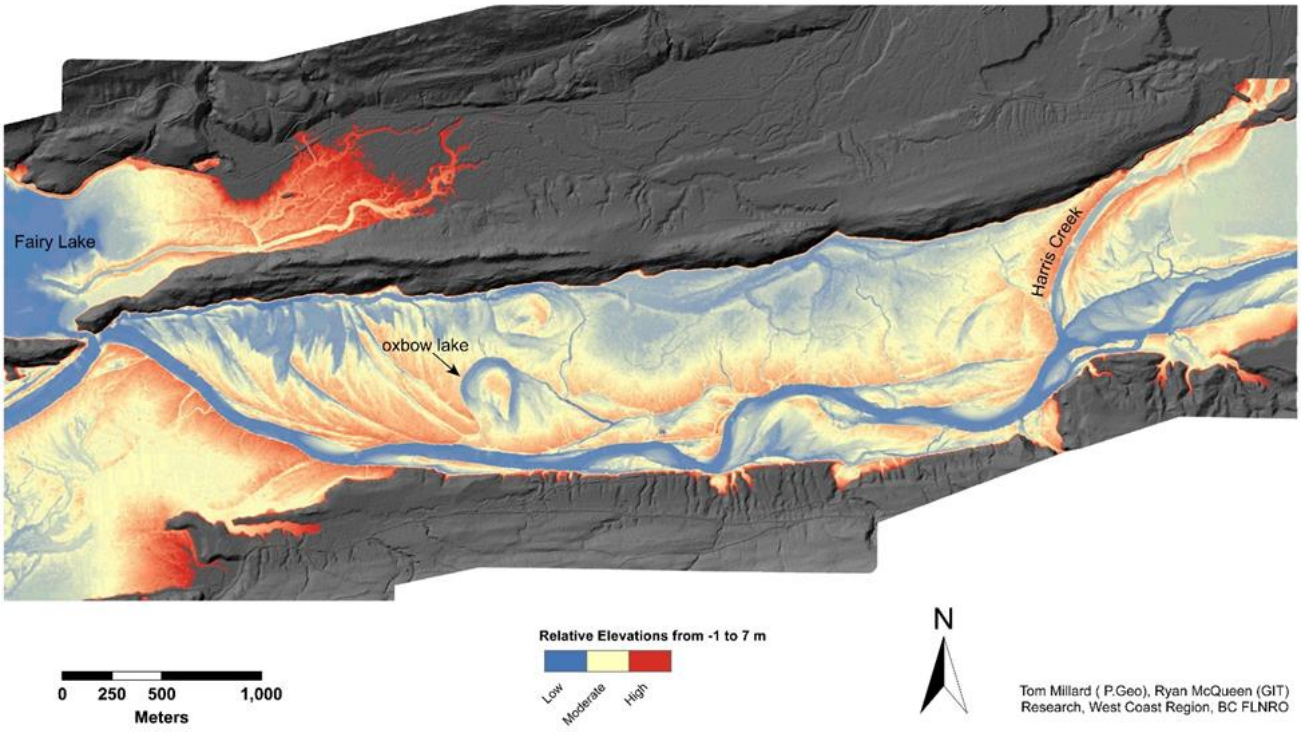

Figure 9: Relative Elevation Model (REM developed for a lower reach section of the San Juan River, Vancouver Island, BC (source: Tim Millard, Research Geomorphologist, BC Ministry of Forests).

3.2 Derivative Product Applications

This section provides examples of how LiDAR derivative products can be applied in a watershed to understand current characteristics (e.g., watershed boundary, stream network) and assess land cover changes over time (e.g., canopy cover) via change detection. These examples are not exhaustive but offer a sense of how LiDAR products can be utilized.

3.2.1 Watershed boundary delineation

Watershed boundaries are lines that represent the drainage divide between adjacent hydrological basins. With LiDAR-derived DEMs, land height is used to determine the steepest path between neighboring pixels. Flow directions are summed into a flow accumulation dataset creating a modelled drainage network that shows the upstream contributing area to all points in a DEM. Users then define a point (called a pour point or watershed outlet), above which to delineate the watershed. The watershed includes all upstream contributing areas of a defined point, as extracted from the modelled drainage network. For example, Figure 10 shows the Carnation Creek Watershed as delineated upstream of the pour point on the western basin edge; all areas in the watershed flow to that outlet according to the DEM. However, the modelled drainage network may not represent the actual watershed's drainage network, particularly for smaller channels. These areas may lack clearly defined stream channels, but based on topographic gradients, will accumulate and contribute water to the downstream drainage network via surface and subsurface pathways.

Higher resolution DEMs tend to produce more detailed and accurate watershed boundary delineations. For example, in Figure 10, the LiDAR-derived watershed boundary is much more detailed than the BC Freshwater Atlas (FWA) boundary which is derived from TRIM data at a 1:20,000 scale. The higher resolution LiDAR dataset captures small topographic variations (e.g., small ridges, depressions) that can influence modelled flow directions and derived drainage network. Higher resolution datasets also present new challenges related to hydrologic conditioning of DEMs, which is the modification of topographic data to more accurately represent the movement of water across a landscape. The process, using software, includes filling sinks or pits, breeching digital dams (infrastructure which block the modeled flow of water across the DEM), and enforcing drainage connections such as culverts, storm sewers, and known tile drainage (Woodrow et al., 2016).

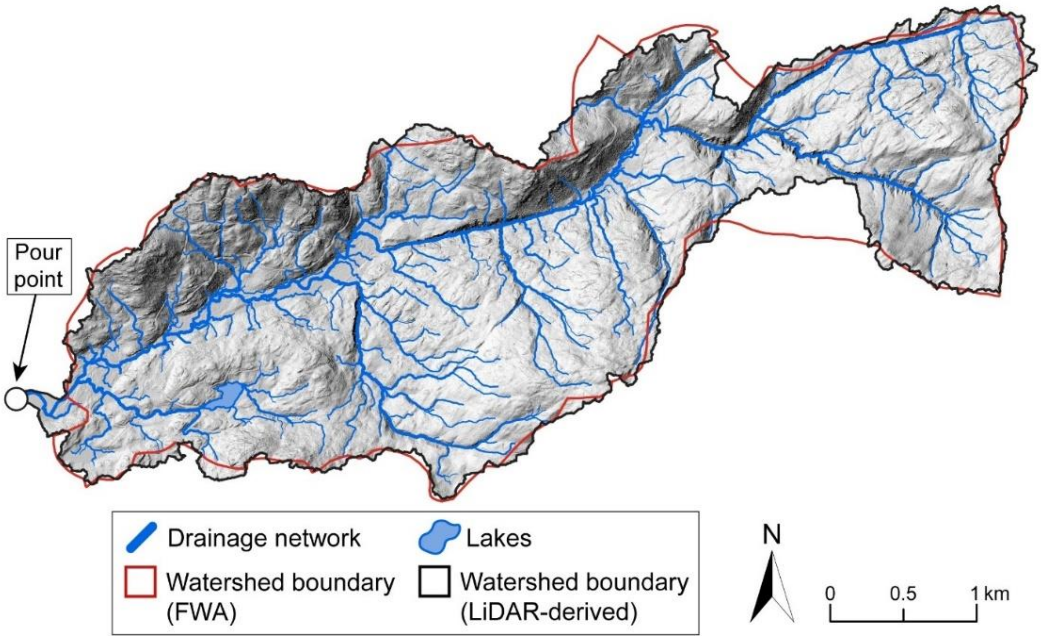

Figure 10: LiDAR derived watershed boundary (black lines) and modelled drainage network (blue lines) for the Carnation Creek Watershed, B.C. Red line displays the watershed boundary available from the BC Freshwater Atlas (FWA).

3.2.2 Stream mapping and ordering

Stream mapping is often integrated with watershed delineation. In this process, users first create flow direction pathways and then convert these into flow accumulations representing the total of all upstream contributing cells. To convert the flow accumulation dataset to a modelled stream network in a GIS program, users must input a threshold, usually a minimum upstream drainage area. Areas with a contributing drainage area below this threshold are not mapped as streams (Whipple and Tucker, 1999).

Stream ordering assigns a numeric order (e.g., first order, second order) to flow junctions in the modelled stream network. This classification helps identify stream types based on branching and understand flow pathways in the drainage network. The Strahler Method (Strahler, 1957) is a stream ordering method where first-order streams are the smallest headwater streams without tributaries. A second order stream begins at the junction of two first order streams and so on downstream to the highest final stream order. Figure 11 illustrates how stream order increases downstream (i.e., to the west).

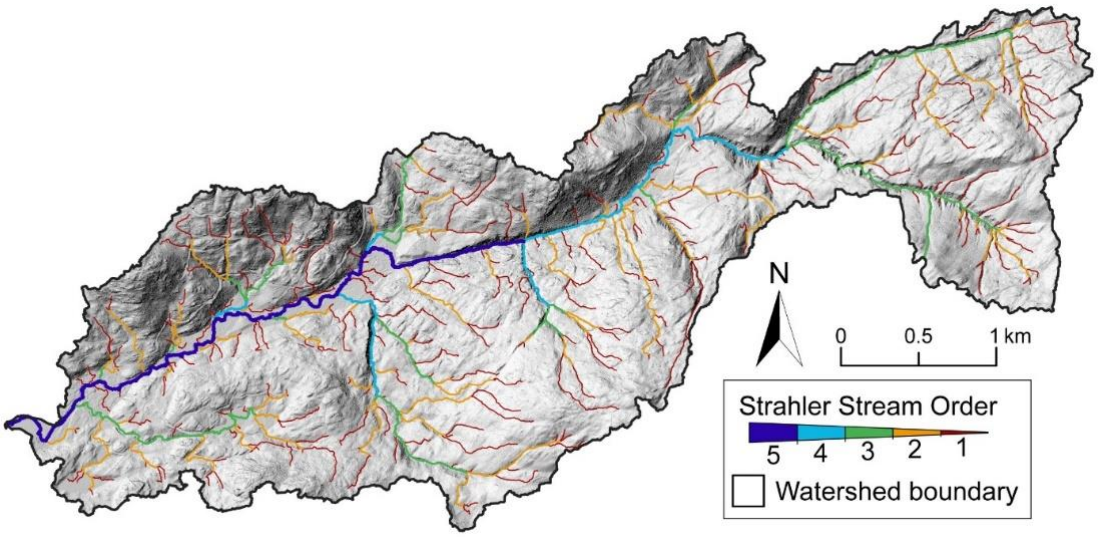

Figure 11: Stream order map generated for the Carnation Creek Watershed, B.C. Streams are modelled and then ordered based on the Strahler method (Strahler, 1957) for stream classification in GIS programs. Note: Modelled streams may or may not be actual streams on the ground.

3.2.3 *Stream channel morphology mapping during low flows*

LiDAR can be used to map stream channel morphology, including slope and shape. Slope describes the gradient of the water surface, side banks, and bedforms such as dunes, bars, and riffle-pool sequences within the stream. Longitudinal channel profiles show the elevation of the water surface or riverbed along a stream reach (upstream/downstream) highlighting a stream's slope. Shape refers to the physical form of the stream channel in plan view (i.e., birds-eye perspective) or as a perpendicular cross-section of the channel. LiDAR can be used to investigate some of these stream channel features. For example, Figure 12 illustrates various stream channel morphology components focussing on channel slope and topography of the floodplain near Carnation Creek.

LiDAR informed mapping of the stream channel's morphology can pinpoint areas at risk of erosion, sedimentation, or landslides, and in some applications, mapping can also identify the presence of large woody debris. Comparison of LiDAR informed mapping collected over different times can show channel changes associated with high flow events.

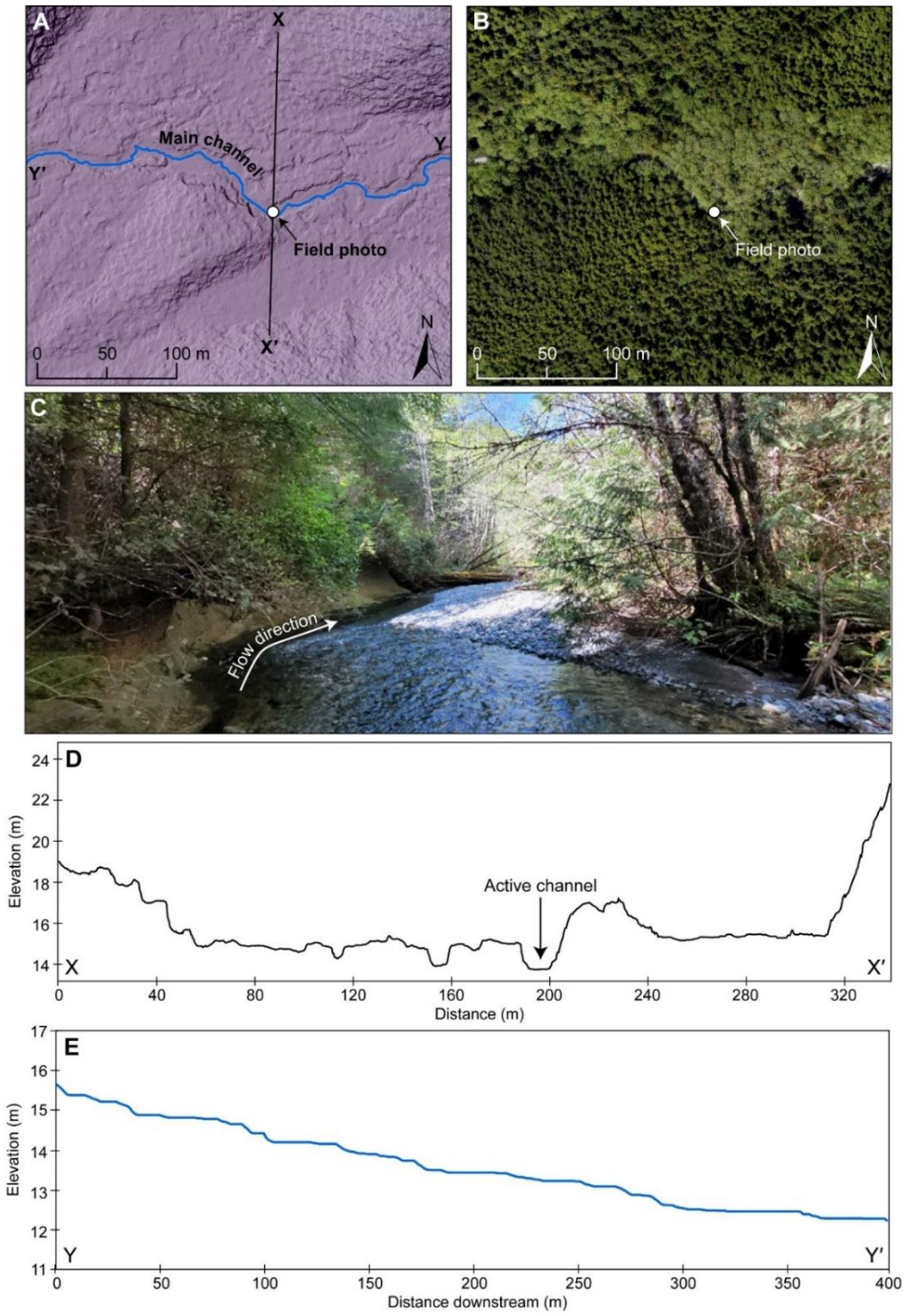

Figure 12: (A) a DEM and (B) matching true colour orthophoto for a section of Carnation Creek Watershed, B.C., (C) a field photo looking downstream from the point of interest, (D) a cross-sectional profile across the mainstem (X to X'), and (E) a channel long profile of the mainstem (Y to Y').

3.2.4 Road and trail mapping

A LiDAR-derived DEM can map roads (Figure 13), trails, and other linear constructed features under forest vegetation that are often hidden in aerial photographs (Hu, 2003). For example, while some roads in Figure 13 appear as lighter green vegetation in the orthophoto (Figure 13B), the road in the northwest section of the image is largely not visible (lacks green vegetation). Conversely, all roads are visible in the LiDAR-derived DEM, including those in the northwest section (Figure 13A). Accurate road mapping can help assess watershed access, enumerate stream crossings, manage roads, and provide information to assess road-related hazards (Duke et al., 2003; White et al., 2010; Ferraz et al., 2016).

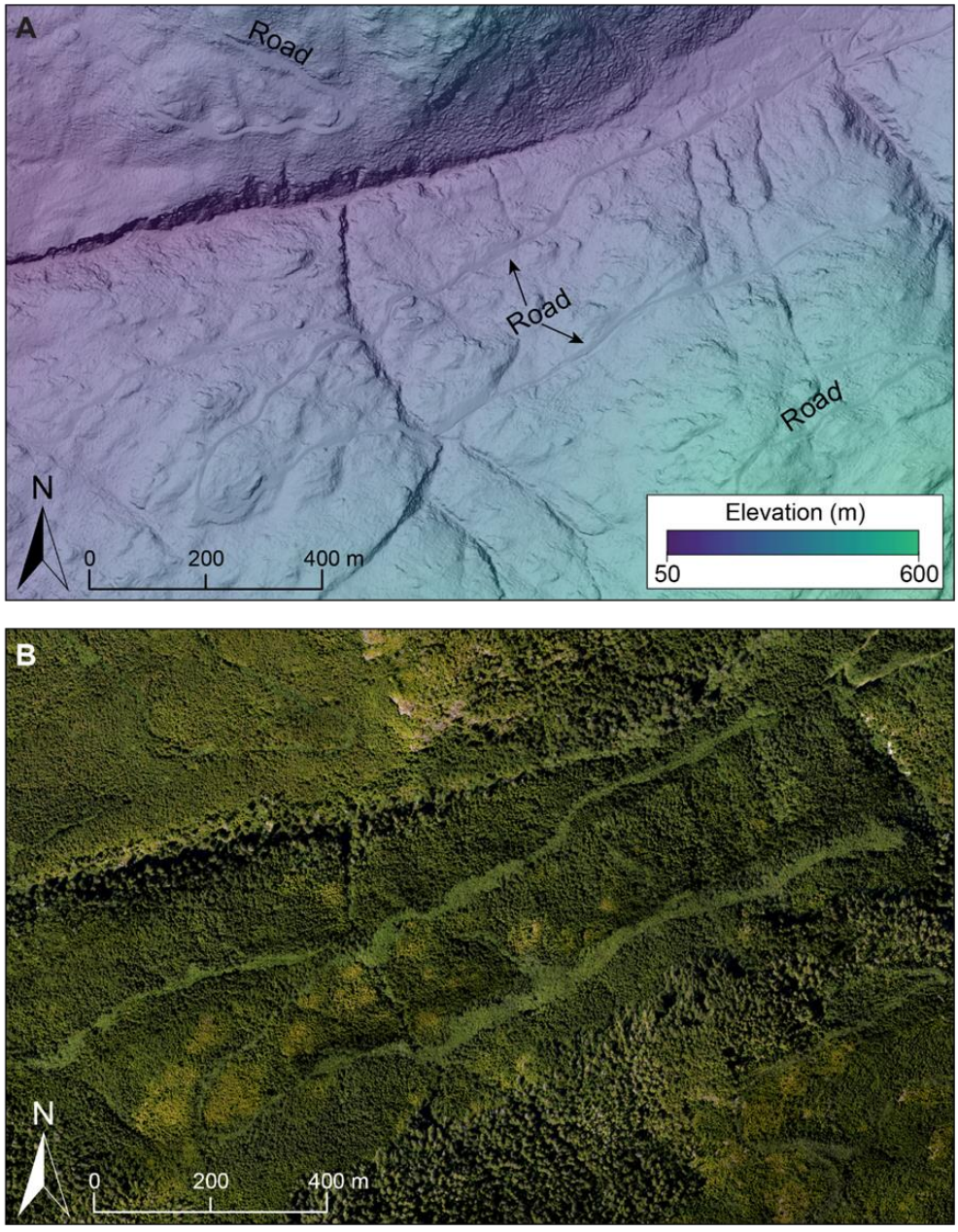

Figure 13: (A) DEM for a portion of the Carnation Creek Watershed, B.C., with roads labelled and (B) a matching, true colour orthophoto for the same area.

3.2.5 Slope and terrain mapping

Understanding how hillslope influences terrain stability is often important in steep and forested watersheds. High resolution, LiDAR-derived slope maps aid in accurately characterizing watershed slopes and identifying potentially unstable terrain. Figure 14 illustrates slope variability in the Carnation Creek Watershed with low slopes concentrated around the downstream and mainstem areas, and steeper slopes in the headwaters.

Since terrain stability is influenced by various factors like surficial geology, vegetation, and surface expression (Howes and Kenk, 1997), LiDAR slope data is typically combined with ground-based survey information to create accurate terrain stability maps. Further information on ongoing hillslope processes (e.g., erosion) and/or other land surface changes in provided in Section *3.2.7 Hillslope processes and land surface changes*.

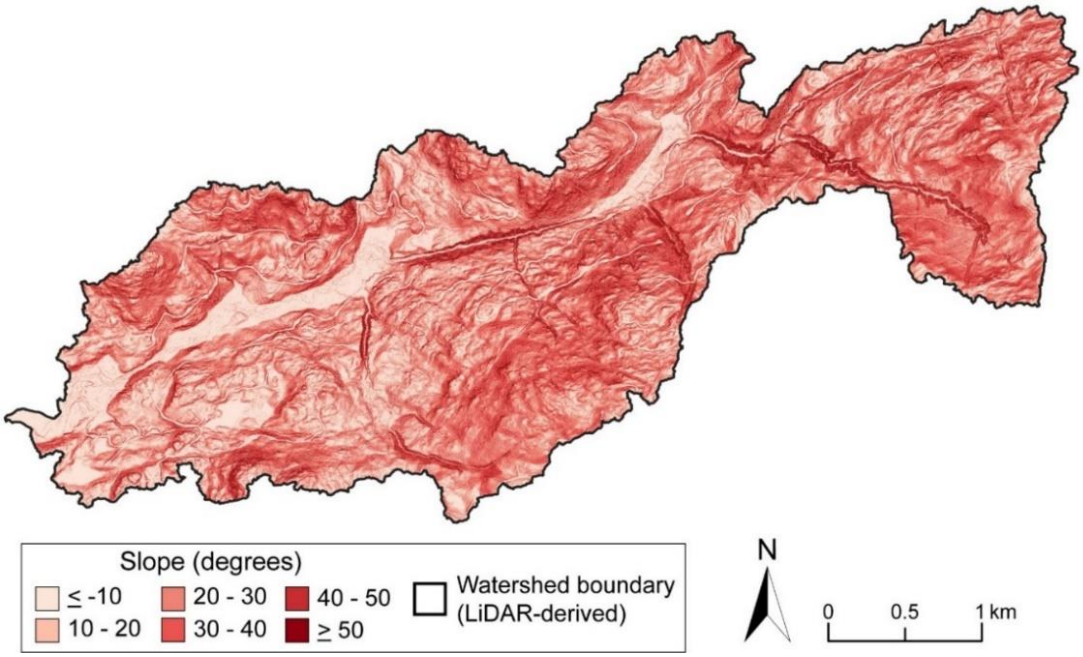

Figure 14: LiDAR-derived slope map of the Carnation Creek Watershed, B.C

3.2.6 Groundwater applications

LiDAR data can be used to assist in mapping the spatial distribution of hydraulic head and groundwater table elevation variability. Such information aids in the interpretation of groundwater gradients, flow directions, fluxes, and velocities, as well as the assessment of surface water and groundwater response to groundwater pumping or aquifer recharge (Healy and Cook, 2002; Von Asmuth et al., 2008; Woessner and Poeter, 2020).

Groundwater levels and well lithologies are measured as depths below ground surface or from the top of the well casing. Accurate elevation measurements at the well head are essential for assessing groundwater processes and aquifer structure. In this context, LiDAR's accuracy provides significant advantages over commonly used DEM products. Figure 15 illustrates the elevation accuracy differences between a DEM developed from a (A) 25-m resolution photogrammetric image and (B) 1-m resolution LiDAR data set. Figure 15C shows ground elevation cross-sections, with the dashed lines representing the photogrammetric image and solid lines representing LiDAR data.

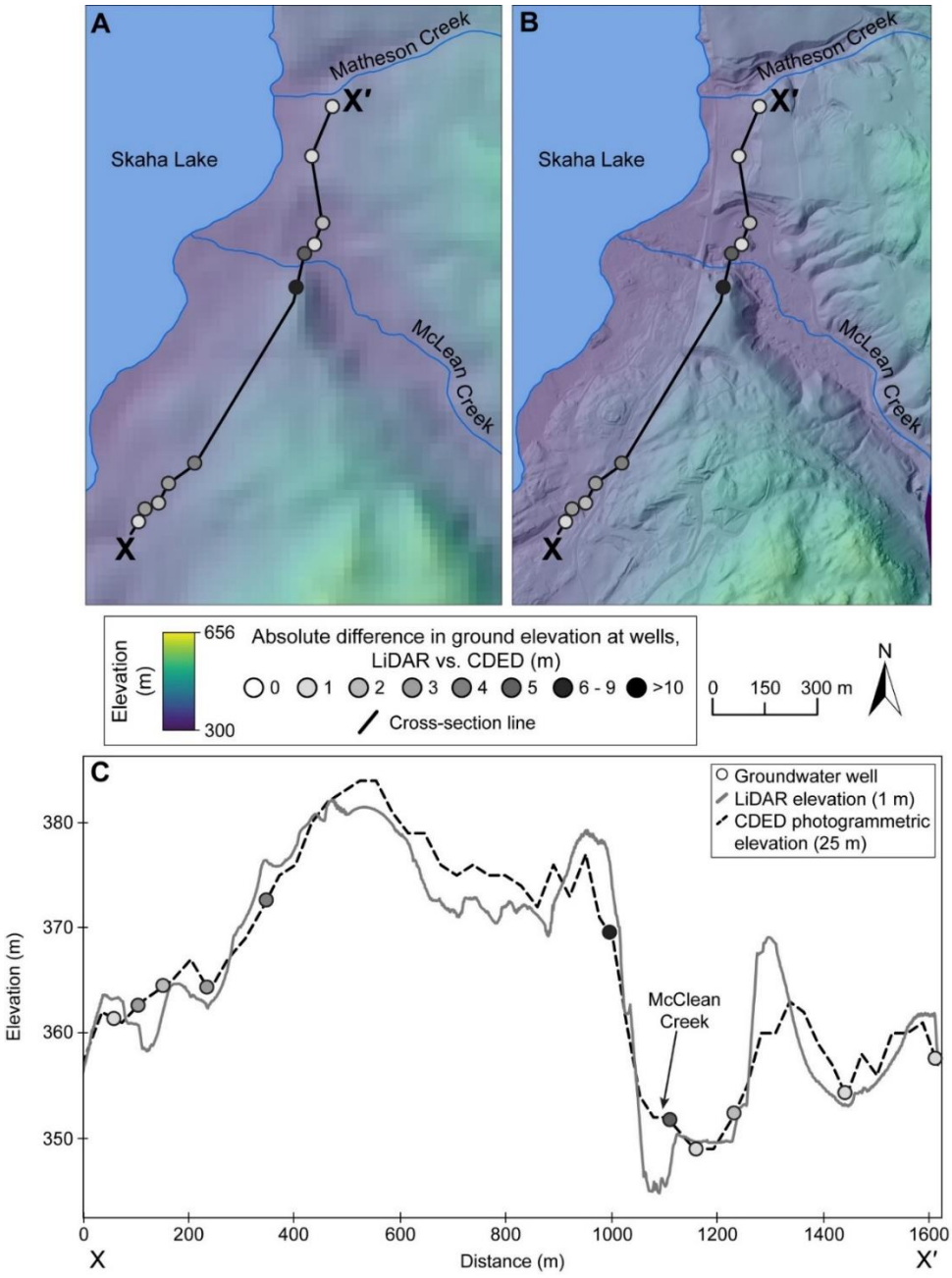

Figure 15: Drainage into Skaha Lake in the Okanagan River Watershed, B.C. and Aquifer 263 with elevation accuracy differences between a DEM developed from a (A) 25-m resolution photogrammetric image and (B) 1-m resolution LiDAR data set. (C) Cross-section showing the reported location of groundwater wells and the difference in their inferred elevations; dashed lines representing the photogrammetric image and solid lines representing LiDAR data.

Elevation differences at each groundwater well range from 0 to 10 m with the greatest difference occurring in the well adjacent to McLean Creek, which would substantially affect the calculation of hydraulic gradients adjacent to the creek and the assessment of surface water and groundwater exchange. Figure 15 shows that the elevation in the photogrammetric image being less accurate and LiDAR providing more precise measurements, emphasizing the importance of accurate ground elevation

for determining groundwater levels. While conventional ground-based methods like surveying can yield precise results, they may not be feasible or cost effective for large hard to access areas.

LiDAR can also be used in groundwater studies to infer shallow groundwater flow characteristics by providing information about watershed surface features such as elevation, slope, and aspect from DEMs and contour maps. LiDAR cannot "see underground" but surface elevation data and topographic mapping can help estimate the groundwater flow direction and identify potential recharge or discharge locations (Cherkauer and Ansari, 2005; Detty and McGuire, 2010; Appels et al., 2016). Since shallow groundwater fluxes in areas with high recharge, flat topography, or low conductivity are primarily driven by topographic gradients rather than pressure head gradients (Condon and Maxwell, 2015) and thus LiDAR can be a valuable tool for estimating groundwater flux.

While LiDAR is valuable for groundwater studies and assessments, it's important to use additional sources of information for a more comprehensive understanding of groundwater characteristics. For example, a LiDAR user investigating groundwater may also collect surficial lithology data (i.e., bedrock geology and unconsolidated surficial materials) to understand how different aquifers might affect groundwater flow interpretation. In areas of multiple aquifers, relying solely on LiDAR data could oversimplify groundwater processes.

3.2.7 Hillslope processes and land surface change assessment

Hillslope processes include continual processes like soil creep, rain splash erosion as well as episodic sudden events such as landslides and debris flows that transport soil, rock, and vegetation materials down slope (Fernandes and Dietrich, 1997; Geertsema et al., 2010; Roering et al., 2001). When collected over different time periods in the same area, differences in two different LiDAR data sets can help quantify the volume and spatial extent of material transported down-slope. As hillslope processes are highly variable in space and time, users need to consider the date and extent of LIDAR data sets for meaningful change detection.

The Chilcotin River Landslide is an example of LiDAR use in British Columbia to understand land surface changes*.* On July 30, 2024, a landslide occurred on the Chilcotin River approximately 30 km upstream from its confluence with the Fraser River. The landslide's material blocked and impounded the Chilcotin River flow for several days. The investigation of its extent used geotechnical assessments, mapping, and modelling, and by remote sensing technology using LiDAR. Two LiDAR datasets, taken on May 20, 2024 (pre-landslide) and July 31, 2024 (post-landslide), were used to create a dataset showing elevation changes due to the landslide (Figure 16).

The landslide deposited material estimated at 1000 m in length, 600 m in width, and 30 m in depth, based on LiDAR elevation change maps from before and after the event (Government of British Columbia, 2024a). LiDAR datasets (pre- and post-landslide DEMs and DEMs of difference) were used to develop hydraulic models that predicted different landslide dam breaching scenarios and estimates of breach timing (Government of British Columbia, 2024b).

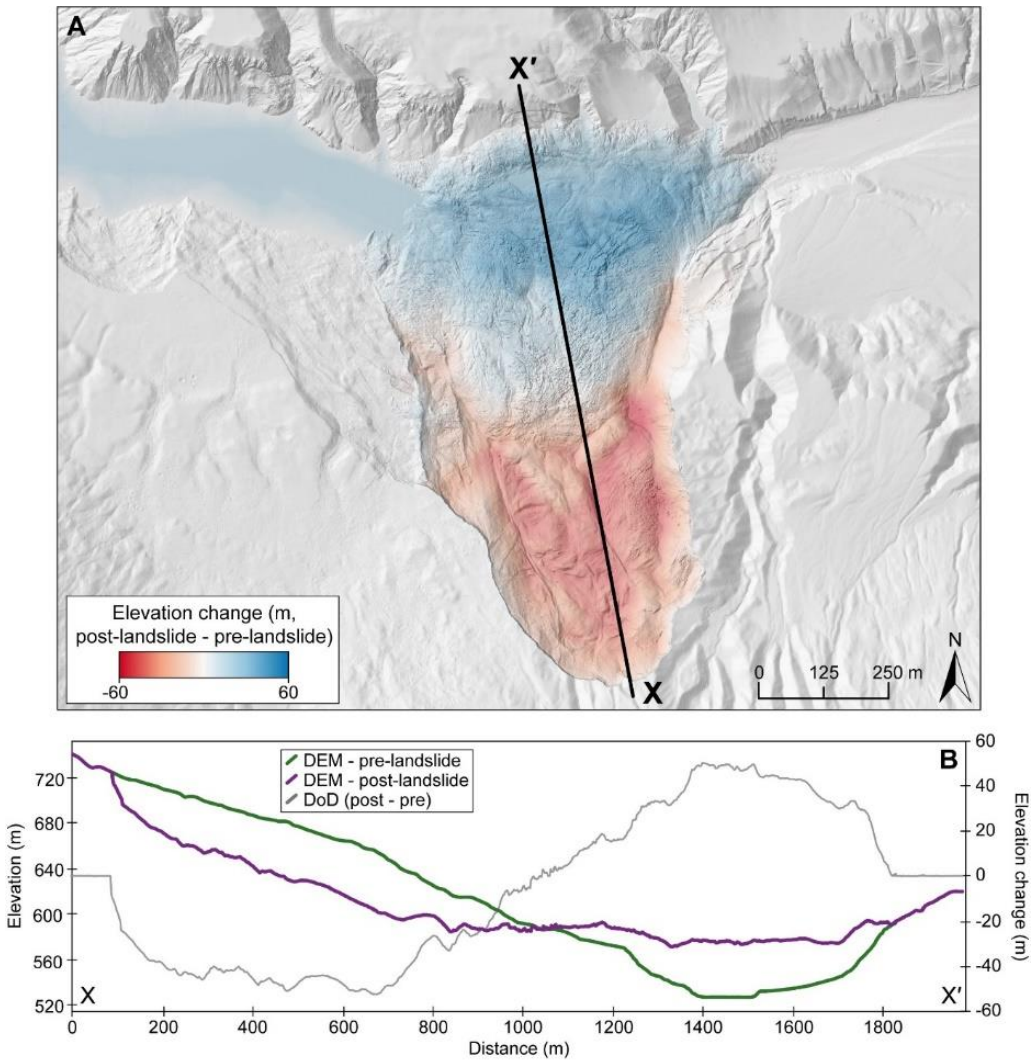

Figure 16: (A) Elevation change (DEM of difference) for the July 30, 2024, Chilcotin River, B.C. slide and (B) cross-section showing the pre-landslide (May 20, 2024) and post-landslide (July 31, 2024) elevation profiles and the DEM of difference (DoD). LiDAR data provided by GeoBC (2024).

3.2.8 Snowpack and glacial change monitoring

LiDAR data from multiple time periods can be used to analyse changes to snow and ice-related features, such as the depth and coverage of snow and glaciers. Snowpack monitoring is essential for managing watersheds in regions where streamflow is dominated by snowmelt. Quantifying annual snowpack accumulation (depth and spatial extent) and long-term trends in snow volume is crucial for water budgets, watershed modelling, and understanding seasonal timing (and changes due to climate) of flow (Dierauer et al., 2021; Bisset et al., 2024). Erosion rates, sediment production, and channel deposition, associated with glaciers can be investigated with LiDAR time-series data (e.g., DEMs of difference).

Figure 17 illustrates how LiDAR data was used to create DEMs for mapping snow depths at Fortress Mountain, AB during February 2018 and April 2019 (Harder et al., 2020a; 2020b). The snow depth is compared to elevation from snow-free conditions in September 2018. The cross-section highlights elevation differences between the snow-on time and the snow-free periods aiding in understanding snow accumulation variations.

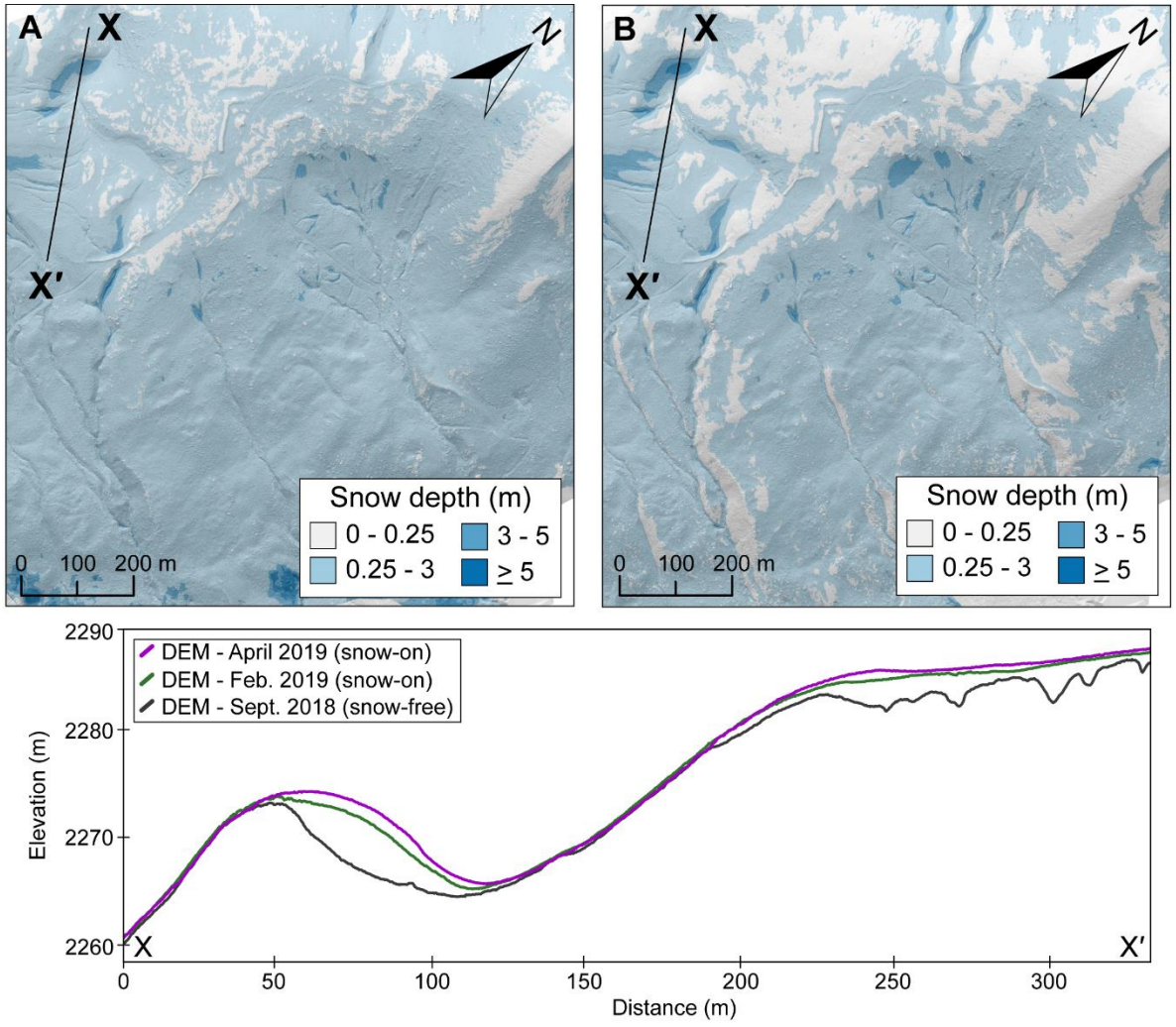

Figure 17: Snow depth at Fortress Mountain, AB in (A) February 2019, (B) April 2019, and (C) a cross-section plots showing the evolution in snow depth compared to snow-free conditions (September 2018). Data source: Harder et al. (2020b).

3.2.9 Canopy Height Model (CHM)

Various land use activities and watershed processes can affect vegetation composition and canopy cover in a watershed. LiDAR data, especially with change detection techniques, can be used to accurately measure and assess these watershed changes.

LiDAR can assist with the following:

- Tree structure, distribution, and composition mapping (e.g., Hyde et al., 2005, Jones et al., 2010; Matasci et al., 2018)
- Tree species classification and forest inventories (e.g., Kwak et al., 2007; Korpela et al., 2010; White et al., 2016, Michałowska and Rapiński, 2021)
- Reforestation and succession planning and monitoring (e.g., Falkowski et al, 2009; van Ewijk et al., 2011; Ahmed et al., 2014; Szostak, 2020)

- Biodiversity and wildlife habitat assessments (e.g., Hyde et al., 2006; Simonson et al., 2014; Guo et al., 2017)
- Wildfire risk assessment and fire-related biomass loss (e.g., Morsdorf et al., 2004; Bolton et al., 2015; Alonzo et al., 2017; Shang et al., 2020)
- Mountain pine beetle impact assessment (e.g., Bater et al., 2010; Niemann et al., 2015)

A Canopy Height Model (CHM) is a LiDAR product used in forest and vegetation studies. It represents tree height by showing the difference between ground and tree top elevations, enabling the mapping of vertical forest structures, and spatial extent of forested areas (Simard et al., 2011). CHMs are useful for predicting aboveground live biomass (Lefsky et al., 2005; Drake et al., 2002; Anderson et al., 2006), primary productivity (Thomas et al., 2008), and biodiversity (Goetz et al., 2007) and is frequently used in forestry and forest management applications.

CHMs from different years help track changes in tree cover due to forestry, forest fires, windstorms, and other events. Figure 18 shows a LiDAR-derived digital surface model of difference (DoD) developed for the Carnation Creek Watershed showing forest stand reduction from 2018 to 2023. The map uses red and blue colours to show elevation changes over time with tree height. The cross-sections in Figure 18 display the elevation data for 2018 (green line) and 2023 (purple line), along with DoD showing the elevation change between these years. This comparison helps visualize how the tree canopy and overall stand coverage have changed over time.

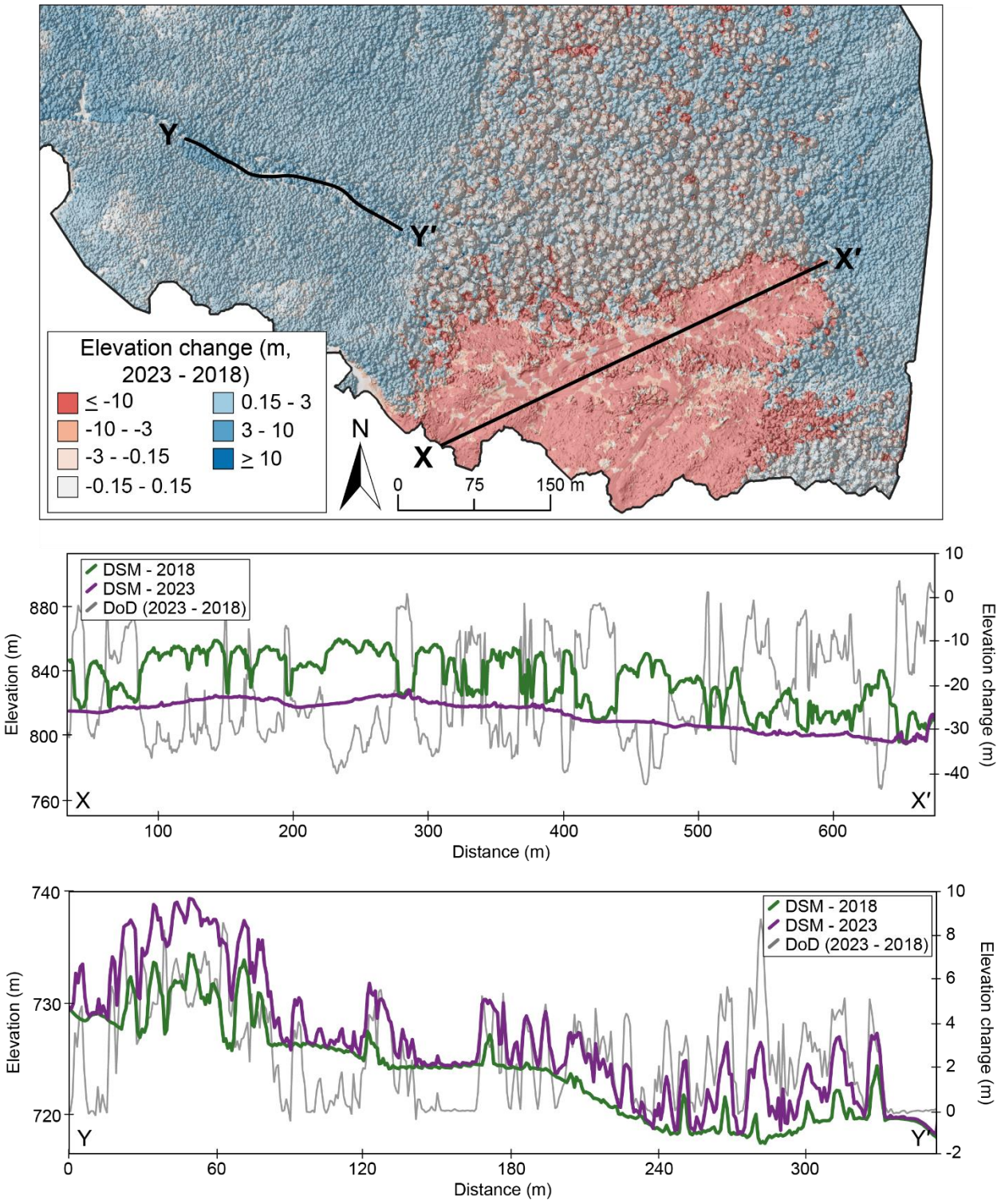

Figure 18: Digital surface model of difference (DoD) between 2023 and 2018 of cut block in Carnation Creek Watershed, B.C. headwaters and two cross-sections.

4. SUMMARY

This report presented an overview of LiDAR data processing, examples of derivative products, and potential limitations (see Section 2.6). It also showcases various applications of LiDAR data across different natural resource sectors with a focus on watershed characterization. LiDAR data does have limitations, and this report outlines several considerations for prospective users. Key challenges highlighted include insufficient computing resources, data storage and sharing, QAQC issues, data gaps, and classification errors. Matching the timing of LiDAR data collection to the specific watershed characterization focus is key. The report stresses the importance of evaluating whether the data collection timeline(s) meets project objectives. However, it does not discuss the costs associated with subsequent and more frequent LiDAR data collection.

Despite a steep-learning curve for new users, LiDAR data offers numerous opportunities for watershed characterization and other natural resource applications. It provides accurate basin scale information making it highly valuable for watershed characterization and other hydrological analyses. Comprehensive spatial data from LiDAR can significantly reduce uncertainty in watershed monitoring, planning, conservation, and restoration decisions in watersheds.

REFERENCES

Ahmed, O.S., Franklin, S.E., and Wulder, M.A. (2014). Interpretation of forest disturbance using a time series of Landsat imagery and canopy structure from airborne lidar. *Canadian Journal of Remote Sensing*. 39(6): 521-542.

Alonzo, M., Morton, D.C., Cook, B.D., Andersen, H.E., Babcock, C., and Pattison, R. (2017). Patterns of canopy and surface layer consumption in a boreal forest fire from repeat airborne lidar. *Environmental Research Letters*, *12*(6): 065004.

Anderson, J., Martin, M.E., Smith, M.L., Dubayah, R.O., Hofton, M.A., Hyde, P., Peterson, B.E., Blair, J.B., and Knox, R.G. (2006). The use of waveform lidar to measure northern temperate mixed conifer and deciduous forest structure in New Hampshire. *Remote Sensing of Environment*, *105*(3): 248-261.

Appels, W.M., Bogaart, P.W., and van der Zee, S.E. (2016). Surface runoff in flat terrain: How field topography and runoff generating processes control hydrological connectivity. *Journal of Hydrology*, 534: 493-504.

Bater, C.W., Wulder, M.A., White, J.C., and Coops, N.C. (2010). Integration of LIDAR and digital aerial imagery for detailed estimates of lodgepole pine (*Pinus contorta*) volume killed by mountain pine beetle (*Dendroctonus ponderosae*). *Journal of Forestry*, 108(3), 111-119.

Bisset, R., Floyd, B., Menounos, B., Bishop, A., Marchenko, S., Marshall, P., and Geospatial, H. (2024). Quantifying snow water storage from aerial LiDAR surveys in eight Pacific coastal watersheds, British Columbia, Canada, EGU General Assembly 2024, Vienna, Austria, 14–19 Apr 2024, EGU24-22543.

Bolton, D.K., Coops, N.C., and Wulder, M.A. (2015). Characterizing residual structure and forest recovery following high-severity fire in the western boreal of Canada using Landsat time-series and airborne lidar data. *Remote Sensing of Environment*, 163: 48-60.

Cavalli, M., Tarolli, P., Marchi, L., and Dalla Fontana, G. (2008). The effectiveness of airborne LiDAR data in the recognition of channel-bed morphology. *Catena*, 73(3): 249-260.

Chawla, I., Karthikeyan, L., and Mishra, A.K. (2020). A review of remote sensing applications for water security: Quantity, quality, and extremes. *Journal of Hydrology*, *585*: 124826.

Chen, Y.H., Mossa, J., and Singh, K.K. (2020). Floodplain response to varied flows in a large coastal plain river. *Geomorphology*, 354: 107035.

Cherkauer, D.S., and Ansari, S.A. (2005). Estimating ground water recharge from topography, hydrogeology, and land cover. *Groundwater*, 43(1): 102-112.

Condon, L.E., and Maxwell, R.M. (2015). Evaluating the relationship between topography and groundwater using outputs from a continental-scale integrated hydrology model. *Water Resources Research*, 51(8): 6602-6621.

Detty, J.M., and McGuire, K.J. (2010). Topographic controls on shallow groundwater dynamics: implications of hydrologic connectivity between hillslopes and riparian zones in a till mantled catchment. *Hydrological Processes*, 24(16): 2222-2236.

Dierauer, J.R., Allen, D.M., and Whitfield, P.H. (2021). Climate change impacts on snow and streamflow drought regimes in four ecoregions of British Columbia. *Canadian Water Resources Journal*: 46(4), 168-193.

Drake, J.B., Dubayah, R.O., Clark, D.B., Knox, R.G., Blair, J.B., Hofton, M.A., Chazdon, R.L., Weishampel, J.F., and Prince, S.D. (2002). Estimation of tropical forest structural characteristics using large-footprint lidar. *Remote Sensing of Environment*, 79: 305-319.

Duke, G.D., Kienzle, S.W., Johnson, D.L., and Byrne, J.M. (2003). Improving overland flow routing by incorporating ancillary road data into digital elevation models. *Journal of Spatial Hydrology*, 3(2): 1-27.

ESRI (2021). What is lidar data? ArcMap – Fundamentals of lidar. https://desktop.arcgis.com/en/arcmap/latest/manage-data/las-dataset/what-is-lidar-data-.htm. Date accessed: January 8, 2025.

Falkowski, M.J., Evans, J.S., Martinuzzi, S., Gessler, P.E., and Hudak, A.T. (2009). Characterizing forest succession with lidar data: An evaluation for the Inland Northwest, USA. *Remote Sensing of Environment*, 113(5): 946-956.

Fernandes, N.F. and Dietrich, W.E. (1997). Hillslope evolution by diffusive processes: The timescale for equilibrium adjustments. *Water Resources Research*, 33(6): 1307-1318.

Ferraz, A., Mallet, C., and Chehata, N. (2016), Large-scale road detection in forested mountainous areas using airborne topographic lidar data, *ISPRS Journal of Photogrammetry and Remote Sensing*, 112: 23-36.

Garbrecht, J., and Martz, L.W. (2000). Digital elevation model issues in water resources modeling. ESRI Proceedings. In: Maidment, D. and Djokic, D. (eds) Hydrologic and Hydraulic Modeling Support with Geographic Information Systems, 1-27. https://proceedings.esri.com/library/userconf/proc99/proceed/papers/pap866/p866.htm. Date accessed: January 8, 2025.

Garousi-Nejad, I., Tarboton, D.G., Aboutalebi, M., and Torres-Rua, A.F. (2019). Terrain analysis enhancements to the height above nearest drainage flood inundation mapping method. *Water Resources Research*, 55(10): 7983-8009.

Gatziolis, D., and Andersen, H.E. (2008). A guide to LIDAR data acquisition and processing for the forests of the Pacific Northwest. USDA Forest Service, Gen. Tech. Rep. PNW-GTR 768: 1-32. https://www.fs.usda.gov/pnw/pubs/pnw_gtr768.pdf. Date accessed: January 8, 2025.

Geertsema, M., Schwab, J.W., Jordan, P., Millard, T.H., and Rollerson, T.P. (2010). Hillslope Processes (Chapter 8). In: Pike, R.G., Redding, T.E., Moore, R.D., Winkler, R.D., and Bladon, K.D. (eds). Compendium of Forest Hydrology and Geomorphology in British Columbia. B.C. Min. For. Range, For.

Sci. Prog., Victoria, B.C. and FORREX Forum for Research and Extension in Natural Resources, Kamloops, B.C. Land Management Handbook 66: 213-273.

GeoBC (2023). Specifications for Digital Elevation Models for the Province of British Columbia. Version 3.0. Issue date: May 5, 2023. Victoria, BC. https://www2.gov.bc.ca/assets/gov/data/geographic/topography/elevation/specifications_for_digital_elevation_models_for_the_province_of_british_columbia_30.pdf. Date accessed: January 8, 2025.

GeoBC (2024). LidarBC's Open LIDAR Data Portal. https://lidar.gov.bc.ca/pages/download-discovery. Date accessed: January 13, 2025.

Goetz, S., Steinberg, D., Dubayah, R., and Blair, B. (2007). Laser remote sensing of canopy habitat heterogeneity as a predictor of bird species richness in an eastern temperate forest, USA. *Remote Sensing of Environment*, 108(3): 254-263.

Government of British Columbia (2024a). Chilcotin River Landslide Information Portal. https://chilcotin-river-landslide-2024-bcgov03.hub.arcgis.com/. Date accessed: January 8, 2025.

Government of British Columbia (2024b). Chilcotin Blockage Situational Last updated: 17:00, August 4, 2024. https://nrs.objectstore.gov.bc.ca/xedyjn/Data/Chilcotin%20River%20Landslide/Chilcotin%20River%20Landslide%20Situation%20Update%20Aug%204.pdf . Date accessed: January 8, 2024.

Greco, S.E., Girvetz, E.H., Larsen, E.W., Mann, J.P., Tuil, J.L., and Lowney, C. (2008). Relative elevation topographic surface modelling of a large alluvial river floodplain and applications for the study and management of riparian landscapes. *Landscape Research*, 33(4): 461-486.

Guo, X., Coops, N.C., Tompalski, P., Nielsen, S.E., Bater, C.W., and Stadt, J.J. (2017). Regional mapping of vegetation structure for biodiversity monitoring using airborne lidar data. *Ecological Informatics*, 38: 50-61.

Hagemann, S., Chen, C., Clark, D.B., Folwell, S., Gosling, S.N., Haddeland, I., Hanasaki, J., Heinke, J., Ludwig, F., Voss, F., and Wiltshire, A.J. (2013). Climate change impact on available water resources obtained using multiple global climate and hydrology models. *Earth System Dynamics*, 4(1): 129-144.

Harder, P., Pomeroy, J.W., and Helgason, W.D. (2020a). Improving sub-canopy snow depth mapping with unmanned aerial vehicles: lidar versus structure-from-motion techniques. *The Cryosphere*, 14(6): 1919-1935.

Harder, P., Pomeroy, J., and Helgason, W. (2020b). Unmanned aerial vehicle structure from motion and lidar data for sub-canopy snow depth mapping. Federated Research Data Repository. https://doi.org/10.20383/101.0193.

Healy, R.W., and Cook, P.G. (2002). Using groundwater levels to estimate recharge. *Hydrogeology Journal*, 10:91-109.

Hiller, J.K., and Smith, M. (2008). Residual relief separation: digital elevation model enhancement for geomorphological mapping. *Earth Surface Processes and Landforms*, 33(14): 2266-2276.

Höfle, B., and Rutzinger, M. (2011). Topographic airborne LiDAR in geomorphology: A technological perspective. *Zeitschrift fur Geomorphologie-Supplementband*, 55(2): 1-29.

Howes, D.E., and Kenk, E. (1997). Terrain Classification System for British Columbia (version 2). B.C. Ministry of Environment, Recreational Fisheries Branch, and B.C. Ministry of Crown Lands, Surveys and Resource Mapping Branch, Victoria, B.C. https://www2.gov.bc.ca/assets/gov/environment/natural-resource-stewardship/nr-laws-policy/risc/terclass_system_1997.pdf. Date accessed: January 8, 2025.

Hu, Y. (2003). Automated extraction of digital terrain models, roads and buildings using airborne LiDAR data. Ph.D. Dissertation. University of Calgary, Department of Geomatics Engineering. https://www.researchgate.net/publication/234478566_Automated_extraction_of_digital_terrain_models_roads_and_buildings_using_airborne_lidar_data. Date accessed: January 13, 2024.

Hyde, P., Dubayah, R., Peterson, B., Blair, J.B., Hofton, M., Hunsaker, C., Knox, R., and Walker, W. (2005). Mapping forest structure for wildlife habitat analysis using waveform lidar: Validation of montane ecosystems. *Remote Sensing of Environment*, 96(3-4): 427-437.

Hyde, P., Dubayah, R., Walker, W., Blair, J. B., Hofton, M., and Hunsaker, C. (2006). Mapping forest structure for wildlife habitat analysis using multi-sensor (LiDAR, SAR/InSAR, ETM+, Quickbird) synergy. *Remote Sensing of Environment*, 102(1-2): 63-73.

Jones, K.L., Poole, G.C., O'Daniel, S.J., Mertes, L.A., and Stanford, J.A. (2008). Surface hydrology of low-relief landscapes: Assessing surface water flow impedance using LIDAR-derived digital elevation models. *Remote Sensing of Environment*, 112(11): 4148-4158.

Jones, T.G., Coops, N.C., and Sharma, T. (2010). Assessing the utility of airborne hyperspectral and LiDAR data for species distribution mapping in the coastal Pacific Northwest, Canada. *Remote Sensing of Environment*, 114(12): 2841-2852.

Kinzel, P.J., Legleiter, C.J., and Nelson, J.M. (2013). Mapping river bathymetry with a small footprint green LiDAR: applications and challenges. *JAWRA Journal of the American Water Resources Association,* 49(1): 183-204.

Korpela, I., Ørka, H.O., Maltamo, M., Tokola, T., and Hyyppä, J. (2010). Tree species classification using airborne LiDAR–effects of stand and tree parameters, downsizing of training set, intensity normalization, and sensor type. *Silva Fennica*, 44(2): 319-339.

Kwak, D.A., Lee, W.K., Lee, J.H., Biging, G.S., and Gong, P. (2007). Detection of individual trees and estimation of tree height using LiDAR data. *Journal of Forest Research*, 12: 425-434.

Lefsky, M.A., Hudak, A.T., Cohen, W.B., and Acker, S.A. (2005). Geographic variability in lidar predictions of forest stand structure in the Pacific Northwest. *Remote Sensing of Environment*, 95(4): 532-548.

Leshchinsky, B.A., Olsen, M.J., and Tanyu, B.F. (2015). Contour Connection Method for automated identification and classification of landslide deposits, *Computers and Geoscience*, 74: 27-38.

Lind, A. (2024). Relative Elevation Models in Global Mapper. Blue Marble Graphics. https://www.bluemarblegeo.com/blog/relative-elevation-models-in-global-mapper/. Date accessed: January 13, 2025.

Lopez, S.R. and Maxwell, R.M. (2016). Identifying urban features from LiDAR for a high resolution urban hydrologic model. *Journal of the American Water Resources Association*, 52(3): 756-768.

Matasci, G., Coops, N.C., Williams, D.A., and Page, N. (2018). Mapping tree canopies in urban environments using airborne laser scanning (ALS): A Vancouver case study. *Forest Ecosystems*, *5*(1): 31.

Michałowska, M., and Rapiński, J. (2021). A review of tree species classification based on airborne LiDAR data and applied classifiers. *Remote Sensing*, 13(3): 353.

Moore, I.D., Grayson, R.B., and Ladson, A.R. (1991). Digital terrain modelling: a review of hydrological, geomorphological, and biological applications. *Hydrological processes*, 5(1): 3-30.

Morsdorf, F., Meier, E., Kötz, B., Itten, K. I., Dobbertin, M., and Allgöwer, B. (2004). LIDAR-based geometric reconstruction of boreal type forest stands at single tree level for forest and wildland fire management. *Remote Sensing of Environment*, 92(3): 353-362.

Ministry of Water, Land, and Resource Stewardship (2024). Provincial lidar program. LidarBC. https://lidar.gov.bc.ca/pages/program. Date accessed: January 13, 2025.

Münzinger, M., Prechtel, N., and Behnisch, M. (2022), Mapping the urban forest in detail: From LiDAR point clouds to 3D tree models. *Urban Forestry and Urban Greening*, 74: 127637.

NOAA Coastal Services Center (2012). Lidar 101: An Introduction to Lidar Technology, Data, and Applications. Revised. Charleston, SC: NOAA Coastal Services Center. https://coast.noaa.gov/data/digitalcoast/pdf/lidar-101.pdf. Date accessed: January 14, 2025.

Niemann, K.O., Quinn, G., Stephen, R., Visintini, F., and Parton, D. (2015). Hyperspectral remote sensing of mountain pine beetle with an emphasis on previsual assessment. *Canadian Journal of Remote Sensing*, 41(3): 191-202.

Notebaert, B., Verstraeten, G., Govers, G., and Poesen, J. (2009). Qualitative and quantitative applications of LiDAR imagery in fluvial geomorphology. *Earth Surface Processes and Landforms*, 34(2): 217-231.

Petroselli, A. (2012). LIDAR data and hydrological applications at the basin scale. *GIScience & Remote Sensing*, 49(1): 139-162.

Powers, P.D., Helstab, M., and Niezgoda, S.L. (2019). A process-based approach to restoring depositional river valleys to Stage 0, an anastomosing channel network. *River Research and Applications*, 35(1): 3-13.

Priestnall, G., Jaafar, J., and Duncan, A. (2000), Extracting urban features from LiDAR digital surface models. *Computers, Environment and Urban Systems*, 24(2):65-78.

Reusser, L., and Bierman, P. (2007). Accuracy assessment of LiDAR-derived DEMs of bedrock river channels: Holtwood Gorge, Susquehanna River. *Geophysical Research Letters*, 34(23): L23S06.

Roering, J.J., Kirchner, J.W., Sklar, L.S., and Dietrich, W.E. (2001). Hillslope evolution by nonlinear creep and landsliding: An experimental study. *Geology*, 29(2): 143-146.

Shang, C., Wulder, M.A., Coops, N.C., White, J.C., and Hermosilla, T. (2020). Spatially-explicit prediction of wildfire burn probability using remotely-sensed and ancillary data. *Canadian Journal of Remote Sensing*, 46(3): 313-329.

Simard, M., Pinto, N., Fisher, J.B., and Baccini, A. (2011). Mapping forest canopy height globally with spaceborne lidar. *Journal of Geophysical Research: Biogeosciences*, 116(G04021), 1-12.

Simonson, W.D., Allen, H.D., and Coomes, D.A. (2014). Applications of airborne lidar for the assessment of animal species diversity. *Methods in Ecology and Evolution*, 5(8), 719-729.

Strahler, A. N. (1957). Quantitative analysis of watershed geomorphology. *Eos, Transactions American Geophysical Union*, 38(6): 913-920.

Szafarczyk, A., and Toś, C. (2022). The use of green laser in LiDAR bathymetry: State of the art and recent advancements. *Sensors*, 23(1): 292.

Szostak, M. (2020). Automated land cover change detection and forest succession monitoring using LiDAR Point Clouds and GIS analyses. *Geosciences*, 10(8): 321.

Thomas, R. Q., Hurtt, G.C., Dubayah, R., and Schilz, M.H. (2008). Using lidar data and a height-structured ecosystem model to estimate forest carbon stocks and fluxes over mountainous terrain. *Canadian Journal of Remote Sensing*, 34(sup2), S351-S363.

Van Den Eeckhaut, M., Poesen, J., Verstraeten, G., Vanacker, V., Nyssen, J., Moeyersons, J., van Beek, L.P.H., and Vandekerckhove, L. (2007). Use of LIDAR-derived images for mapping old landslides under forest, *Earth Surface Process and Landforms*, 32: 754-769.

van Ewijk, K.Y., Treitz, P.M., and Scott, N.A. (2011). Characterizing forest succession in Central Ontario using LiDAR-derived indices. *Photogrammetric Engineering and Remote Sensing*, 77(3): 261-269.

Von Asmuth, J.R., Maas, K., Bakker, M., and Petersen, J. (2008). Modeling time series of ground water head fluctuations subjected to multiple stresses. *Groundwater*, 46(1):30-40.

Walker, J.P., and Willgoose, G.R. (1999). On the effect of digital elevation model accuracy on hydrology and geomorphology. *Water Resources Research*, 35(7): 2259-2268.

Whipple, K.X. and Tucker, G.E. (1999). Dynamics of the stream-power river incision model: Implications for the height of mountain ranges, landscape response timescales, and research needs. *Journal of Geophysical Research,* 104(B8): 17661-17764.

White, R.A., Dietterick, B.C., Mastin, T., and Strohman, R. (2010). Forest roads mapped using LiDAR in steep forested terrain. *Remote Sensing*, 2(4): 1120-1141.

White, J.C., Coops, N.C., Wulder, M.A., Vastaranta, M., Hilker, T., and Tompalski, P. (2016). Remote sensing technologies for enhancing forest inventories: A review. *Canadian Journal of Remote Sensing*, 42(5): 619-641.

Woessner, W.W., and Poeter, E.P. (2020). Hydrogeologic Properties of Earth Materials and Principles of Groundwater Flow. The Groundwater Project, Guelph, ON. https://books.gw-project.org/hydrogeologic-properties-of-earth-materials-and-principles-of-groundwater-flow/chapter/mapping-the-head-distribution/. Date accessed: January 14, 2025.

Wolock, D.M., and Price, C.V. (1994). Effects of digital elevation model map scale and data resolution on a topography-based watershed model. *Water Resources Research*, 30(11): 3041-3052.

Woodrow, K., Lindsay, J.B., and Berg, A.A. (2016). Evaluating DEM conditioning techniques, elevation source data, and grid resolution for field-scale hydrological parameter extraction. *Journal of Hydrology*, 540: 1022-1029.

Wu, Q. and Lane, C.R. (2017), Delineating wetland catchments and modelling hydrologic connectivity using LiDAR data and aerial imagery, *Hydrology and Earth Systems Sciences*, 21: 3579-3595.

Yang, D., Yang, Y., and Xia, J. (2021). Hydrological cycle and water resources in a changing world: A review. *Geography and Sustainability*, 2(2): 115-122.